

26 decomposition rates among forest disturbance classes, structural equation models
27 revealed significant indirect pathways, where anthropogenic canopy openness altered
28 microclimatic conditions which in turn suppressed decomposer activity, such as termites,
29 a key biotic driver of decomposition. Our findings provide novel experimental evidence
30 that forest structure and microclimate mediate the role of decomposers in carbon cycling,
31 emphasizing the need to incorporate functional wood traits and indirect disturbance
32 effects into carbon models to better predict ecosystem responses under increasing forest
33 degradation and climate change.

34 **Keywords:** Amazon, wood decomposition, selective logging, forest fires, termites, fungi,
35 microclimate.

36 ** The abstract in Portuguese is available in the Supplementary Material

37

38 **Highlights**

- 39 • Wood decay was not affected by broad forest degradation classes
- 40 • Structural models effectively untangled direct and indirect drivers of wood decay
- 41 • Canopy openness and microclimate indirectly affect decomposition via
42 decomposers
- 43 • Termites and wood density shaped decomposition across forest disturbance
44 gradients

45

46

47

48

49 **1. Introduction**

50 Tropical rainforests are important to global carbon dynamics (Pan et al., 2011).
51 These ecosystems take up only 12% of the Earth's surface, yet they account for ~40% of
52 terrestrial net primary production, holding 25% of the world's carbon stocks (Townsend
53 et al., 2011). While growth is important for defining live biomass, necromass also
54 represents a major carbon pool. In tropical forests, around 8% of total carbon stocks and
55 14-19% of the annual CO₂ flux ties up forest necromass (Palace et al., 2008; Pan et al.,
56 2011), which is defined as dead woody plant material, including trunks, branches, leaves,
57 roots and dead standing or fallen logs (Harmon et al., 1986). The fate of necromass,
58 through decomposition, is a crucial yet understudied process governing carbon
59 persistence or release in forest ecosystems (Giardina, 2019).

60 Within tropical forests, previous research has identified three major factors that
61 influence dead wood decomposition rates. First, wood characteristics directly influence
62 decomposition rates, with species with lower wood density being more rapidly
63 decomposed than those with high wood density levels (Chambers et al., 2000; Mori et al.,
64 2014; Dossa et al., 2020). Second, the presence of termites is important, and leads to
65 significant increases in decomposition rates (Dossa et al., 2020; Seibold et al., 2021) - for
66 example, in Malaysian forests termites were responsible for 58-64% of wood
67 decomposition, while microbes contributed between 36-42% (Griffiths et al., 2021).
68 Third, climate plays an important role by regulating decomposer activity (Bradford et al.,
69 2014; Ewers et al., 2015). For example, Wijas et al. (2024) showed that microclimate
70 limits decomposition by microbes in dry periods, while termite activity remained stable
71 throughout the year in Australian forests.

72 However, these decomposition drivers are dynamic and influenced by
73 anthropogenic disturbance. Human activities such as logging, fire and their interactions

74 degrade tropical forest structure, often resulting in hotter and drier understory and forest
75 floor environments (Hardwick et al., 2015; Jucker et al., 2018; Marsh et al., 2022).
76 Additionally, anthropogenic disturbance in tropical forests frequently shifts tree species
77 composition toward early-successional or pioneer species, which tend to have lower wood
78 density (Berenguer et al., 2018; Pinho et al., 2024). This compositional shift alters the
79 quality of the necromass pool, potentially accelerating decomposition due to the
80 prevalence of more labile substrates. These changes may also influence decomposer
81 efficiency via the “home field advantage” (HFA) mechanism, in which decomposers are
82 more effective at processing wood types that are locally abundant and familiar (Wu et al
83 2024).

84 Despite recent advances in understanding decomposition processes in forest
85 ecosystems (Harmon et al., 2020; Russel et al., 2015), mechanistic frameworks linking
86 forest disturbance to decomposition dynamics - particularly through direct and indirect
87 pathways - remain scarce, mainly for tropical forest. While a few such approaches have
88 been applied in temperate and subtropical ecosystems (Risch et al., 2022; Wu et al., 2021),
89 they are even rarer in studies addressing degraded or human-modified tropical forests
90 (Harmon et al., 2020). This gap is particularly concerning in the Amazon, where over 1
91 million km² of Amazonian forests are human modified (Lapola et al., 2023), a figure that
92 will continue to increase. Climate predictions also show that extreme droughts and
93 subsequent forest fires will become more frequent (Duffy et al., 2015; Fonseca et al.,
94 2019), which may further accelerate carbon loss from necromass. Understanding how
95 disturbance alters deadwood turnover is thus crucial for anticipating changes in regional
96 and global carbon dynamics (Martin et al., 2021; Seibold et al., 2021).

97 In order to enhance our understanding of wood decomposition in human-modified
98 tropical forests, we conducted a year-long decomposition experiment to investigate how

99 forest disturbance affects wood decomposition in the eastern Amazon. We assessed
100 microclimatic, biotic, and site-specific variables to investigate the decomposition rates of
101 15 Amazonian tree species, selected to represent a gradient of wood densities from
102 pioneers to old-growth species. We use the experimental approach to answer four specific
103 research questions: (Q1) How do rates of wood decomposition differ across forest
104 disturbance classes, species, and over time? (Q2) How do the microclimatic changes
105 resulting from forest disturbance affect wood decomposition, and is there an interaction
106 with species wood density? (Q3) Is the prevalence of observed termite attack and fungal
107 proliferation explained by structural (wood density), site-specific (canopy openness) and
108 microclimatic variables? Finally, we combine all data to ask: (Q4) What are the direct
109 and indirect controls on rates of wood decomposition in human-modified tropical forests?

110 **2. Methods**

111 *2.1. Study area*

112 The study was carried out in the municipalities of Santarém, Belterra and Mojuí
113 dos Campos (hereafter, Santarém region), located in the eastern Brazilian Amazon (Fig.
114 SM 1). The region holds a heterogeneous mix of undisturbed and disturbed forests that
115 have suffered from selective logging and forest fires in the past (Berenguer et al., 2021;
116 Gardner et al., 2013) and is representative of other regions of the Amazon (Berenguer et
117 al., 2014; Bullock et al., 2020). The regional climate is warm and humid, with an annual
118 mean temperature of 27.12°C between the years 2000 and 2023 (Alvares et al., 2013;
119 INMET, 2025) and receives an average rainfall of 2000 mm per year, with a marked dry
120 season usually occurring between July and November (Andrade and Corrêa, 2014;
121 Restrepo-Coupe et al., 2013).

122

123 *2.2. Species selection and preparation*

124 We selected 15 broad-leaved Amazonian tree species distributed along a gradient
125 of wood density, from pioneers (0.36 g.cm^{-3}) to old-growth species (1.15 g.cm^{-3} – Table
126 SM 1). We used a local sawmill to cut 216 individual uniform blocks of bark-free wood
127 for each species, with blocks measuring 10 x 3 x 3 cm. Blocks were mostly from the
128 heartwood of the main trunk, although we controlled for variation between blocks by
129 measuring the wood density of each individual piece ($n = 3240$ measurements). To do
130 this, each block was first oven dried at $80 \text{ }^\circ\text{C}$ until it reached a constant weight. Each
131 species had a different time to confirm constant weight (Table SM 2). After weighing,
132 the volume of each block was calculated using the gravimetric water displacement
133 method (ASTM, 2008). The wood density for each block was then calculated by dividing
134 the mass by the volume displaced. As opposed to the basic method of estimating wood
135 density (Fearnside, 1997; Nogueira et al., 2005), we measured the volume of each piece
136 of wood after oven drying; this was necessary as the samples came from the local sawmill,
137 and it was not possible to standardize their initial moisture content. As such, the density
138 values were likely to overestimate the true density compared to global datasets based on
139 green volumes (Zanne et al., 2009) but were internally consistent within this study and
140 were highly correlated with global dataset ($r=0.9734$; $t=15.343$; $df=13$, $P<0.001$ – Fig.
141 SM 2). Finally, we used a wire to group the blocks on collars, each containing one block
142 from each species (Fig. SM 3). Blocks were placed in a random order to avoid any
143 consistent ‘neighbour’ effects, which would influence decomposition rates of adjacent
144 blocks if any one species was more attractive to decomposers.

145

146

147 2.3. *Measuring decomposition in the forest*

148 We established 18 transects that were 300 m long, distributed along a gradient of
149 pre-El Niño forest disturbance, including: undisturbed (UF), selectively logged (Logged)
150 and logged-and-burned (LBF) forests. During the 2015-2016 El Niño, nine transects were
151 only affected by drought (EN-drought, hereafter), while the other nine were also affected
152 by fires, burning between the last week of November 2015 and the first of January 2016.
153 We used the term “EN-fire” for these plots but recognize that they suffered both drought
154 and fire effects. Thus, our study encompassed three $UF_{ENdrought}$ ($n = 3$), three $Log_{ENdrought}$
155 ($n = 3$), three UF_{ENfire} ($n = 3$), three $LBF_{ENdrought}$ ($n = 3$) and six LBF_{ENfire} ($n = 6$) transects
156 (Fig. SM 1). Transects were located in *terra firme* forests, at least 100 meters from the
157 forest edge, and with a minimum distance of 1500 meters between each other. The same
158 transects formed the basis of other work in the region, including Berenguer et al. (2021).

159 In January 2023, during the onset of the wet season, collars were placed on the
160 forest soil surface in each transect. We established three sampling points at 0, 150 and
161 300 m. In each sampling point, we installed four collars located at 1 - 2 m distance from
162 each other (Fig. 1). In total, we installed 216 collars (i.e. 18 transects with 3 sampling
163 points and 4 collars per sampling point). One collar was removed from each sampling
164 point at four-time intervals: three, six, nine and twelve months after the start of the
165 experiment. After being removed from the field, the blocks were oven-dried until they
166 reached a constant weight for each species (Table SM 2). Prior to drying, any external
167 soil adhering to the blocks was removed. Data from two LBF_{ENfire} transects in the last
168 removal period (after twelve months) were excluded from the analyses, as these transects
169 burned again during this experiment, leading to the loss of the collars.

170

171

172 2.4 *Environmental predictors of decomposition*

173 Microclimatic, biotic and site-specific variables were recorded monthly along the
174 studied transects during the experiment. For microclimate, we recorded air temperature
175 (°C) and relative humidity (%) at each sampling point with a Kestrel DROP D2 data
176 logger (accuracy of 0.5° and 2%, respectively). Loggers were placed five centimeters
177 aboveground and among the four collars present at each sampling point (Fig. 1), recording
178 microclimate data every 10 minutes. Every month, we gathered data from the loggers and
179 removed any leaf litter that obstructed them. For each logger, we calculated four
180 variables: average air temperature of the hottest period (11 - 17h); average air temperature
181 during the coldest period (00 - 06h), hereafter *max day* and *min night* temperature,
182 respectively; average temperature range and average relative humidity. *Min night* and
183 *max day* temperatures were calculated by filtering raw data, computing daily averages for
184 each transect, then deriving monthly means. For temperature range, we followed the same
185 method but subtracted the *max day* and *min night* averages for the entire daily period. The
186 average relative humidity per forest class was also quantified using the daily data, then
187 deriving monthly means.

188 For forest structure, we measured canopy openness (%), which represents the
189 fraction of the angular area of the sky that is not obstructed by vegetation when viewed
190 from a given point (Gonsamo et al., 2013). We estimated it by taking one hemispherical
191 photograph per sample point every month (Fig. 1), using a standardized exposure
192 configuration. All hemispherical photographs were taken with a Nikon CoolPix 4500
193 digital camera (4 megapixels). A Nikon LC-ER1 fisheye lens with a 180° field of view
194 was attached to the camera for hemispherical photo acquisition (Hardwick et al., 2015).
195 The camera was mounted on a tripod one meter from the ground and pointing North. At
196 each sample point, all palm leaves, vines or branches \leq 2m from the camera were

197 removed. Photographs were taken always ensuring suitable sky conditions to prevent
198 overexposure and maintain the accuracy of canopy openness calculations. Digital image
199 processing was carried out using Hemisfer software (Schleppi et al., 2007).

200 To track the association between biotic factors and wood decomposition
201 throughout the whole experimental period, the presence of fungi and termites were
202 evaluated visually, assessing each wood block during each monthly field visit, and again
203 before oven-drying for reweighing. The visual assessment of termites involved searching
204 for the presence of galleries with or without fecal material or individual termites in the
205 damaged wood blocks. The presence of fungi was determined by the visual presence of
206 hyphae growth or fruiting bodies, representative of successful colonization and
207 reproduction (Dambros et al., 2020; Dawson et al., 2019; Irbe et al., 2010).

208 2.5. Statistical analysis

209 For each wooden block we calculated their proportional loss of mass by using the
210 equation $PML = (im - fm)/im$, where PML is proportional mass loss; im is initial mass (g);
211 and fm = final mass (g). PML is a dimensionless measurement (from 0 to 1) and expresses
212 the mass loss fraction during an exposure period.

213 To evaluate differences in decomposition across forest classes (Q1), we applied
214 Kruskal-Wallis test, as PML did not show a normal distribution even with data
215 transformations. These comparisons were also conducted across species, for each of the
216 four removal periods (3, 6, 9, and 12 months) and microclimate among forest disturbance
217 classes.

218 To assess the direct pathways, we used generalized linear mixed models
219 (GLMMs). We repeated analysis of cumulative mass loss for each of the four removal
220 periods (after 3, 6, 9 and 12 months); although latter periods included some of the
221 decomposition that occurred in earlier periods, we were interested in assessing if the

222 variables predicting total loss were consistent over time (Oberle et al., 2019). The
223 quarterly averages were appropriate for each predictor variable in the models. For these
224 tests, the Z transformation was used to standardize all predictors. In all models, transect
225 identity (ID) was included as a random factor, accounting for spatial autocorrelation.

226 To test whether microclimatic variation (*max day* and *min night* air temperature,
227 average temperature range and average relative humidity) affects *PML* (Q2), GLMMs
228 with a lognormal distribution were used (*glmmTBM* package; Brooks et al., 2017). The
229 inclusion of the interaction term aimed to test whether species with different wood
230 densities respond differently to microclimatic conditions, thereby assessing potential
231 evidence for a “home field advantage” dynamic. GLMMs with binomial distributions
232 were used to test whether the prevalence of observed termite attack or fungal proliferation
233 was explained by microclimate (Q3). Stepwise backward selection was used to assess the
234 direct pathways of explanatory variables on wood decomposition.

235 For the GLMMs, variables were removed based on AIC until the best-fit model
236 was reached. In lognormal models, all variables in any period were retained for
237 comparability purposes, while non-significant variables in binomial models could not be
238 compared due to model inadequacies. Model diagnostics were conducted using the
239 package *DHARMA* (Hartig, 2016). To ensure the absence of collinearity, the variance
240 inflation factor values for each model were checked (< 5). The *plot_models* function on
241 the *sjPlot* package (Lüdtke, 2013) was used to plot effect sizes and odd ratios of the
242 models.

243 To investigate the direct and indirect pathways by which our variables may affect
244 wood decomposition (Q4), we constructed piecewise Structural Equation Models (SEM)
245 using the *piecewiseSEM* package (Lefcheck, 2016) based on a priori path diagram (Fig.
246 SM 4), in which a structured set of linear models is fitted individually. This approach

247 allowed us to consider all the models generated in our previous questions, including
248 random factors (Transect ID). Given potential biotic interactions (Bradford et al., 2021),
249 we included a correlated error path between termite and fungal presence (Wu et al., 2021).
250 Shipley's d-separation test was used to assess the fit of the model using Fisher's C-statistic
251 (Shipley, 2013). For the results, the standardized coefficients (estimates) scaled by the
252 significant interval were used because the parameter estimates of models with a log-
253 normal distribution could not be standardized by variances (Grace et al., 2012). We
254 refined the original models for each block removal, eliminating non-significant links,
255 starting with the least significant, and continuing gradually until the change in AICc
256 associated with a step was less than 2 units. Since the effects of predictors on wood mass
257 loss are more accurate in the longer-term (Oberle et al., 2019), we carried out the SEM
258 only on our last removal, after twelve months. All statistical analyses were conducted in
259 R version 4.4.0 (R Core Team, 2024).

260 **3. Results**

261 Decomposition of all species, assessed as the average proportional mass loss,
262 increased significantly throughout the year ($\chi^2 = 422.87$, $df = 3$, $p < 0.001$; Fig. 2A), from
263 0.03 ± 0.08 (mean \pm SD) after three months, 0.09 ± 0.16 after six months, 0.15 ± 0.24
264 after nine months to finally 0.21 ± 0.29 after 12 months. There was a high degree of
265 variation in interspecific decomposition ($\chi^2 = 2337.5$, $df = 14$, $p < 0.001$; Fig. 2B). The
266 species with the lowest decomposition rate, over the course of the experiment, was
267 *Handroanthus serratifolius* (0.0065 ± 0.0211), while the highest decomposition rate
268 (0.3939 ± 0.3253) was observed in *Jacaranda copaia*. No significant variation in wood
269 decomposition was observed between forest classes ($\chi^2 = 4.3402$, $df = 4$, $p = 0.36$; Fig.
270 2C) throughout 12 months.

271 *3.1. The effects of woody density, microclimate and canopy openness on wood*
272 *decomposition*

273 Wood density had a strong negative relationship with wood decomposition
274 throughout the experiment (Fig. 3, Table SM 3). Effect sizes for other variables were
275 small in comparison, and not consistent across time periods. After twelve months of
276 decomposition, *max day* temperature showed a negative relationship with wood
277 decomposition, while a greater temperature range enhanced decomposition. The effects
278 of *min night* temperature, relative humidity and canopy openness were not significant,
279 and none of the variables considered had a significant interaction with wood density.
280 These results therefore did not support the existence of a significant “home field
281 advantage” in any of the removal periods, matching the lack of an obvious link between
282 decomposition rates of different wood densities and the forest disturbance class (Fig. SM
283 5).

284 *3.2. The effects of microclimate and biophysical variables on the presence of*
285 *decomposers*

286 The significance of the predictor variables varied over time (Table SM 4; Table
287 SM 5). Microclimate variables showed effects in the initial and middle months of the
288 experiment (Fig. 4). The presence of termites showed a positive association with *max day*
289 temperature, while higher relative humidity favored the appearance of fungi. Temperature
290 range had negative effects in the last two removals only for termites. Wood density was
291 the only variable that showed significance throughout the experimental period, with the
292 presence of termites and fungi mainly observed on low density woods. The odds of
293 finding termites in the experimental blocks were negatively related to the presence of

294 fungi, and vice versa, indicating negative interactive effects between termites and fungi
295 (Table SM 6).

296 3.3. *Direct and indirect drivers of wood decomposition*

297 Wood decomposition was accelerated by the presence of termites, while higher
298 wood densities and the interaction of termites and fungi slowed it down (Fig. 5A and
299 Table SM 6). The inclusion of termites and fungi presence in the model did not alter the
300 minimal influence of microclimatic variables on wood decomposition. Despite the clear
301 microclimatic differences between forest classes (Table SM 7), the only microclimate
302 variable to show a significant effect was the average temperature range after twelve
303 months, but the effect size remained small compared to other variables (Fig. 5B). Canopy
304 openness was also significant only in the last removal, but with a negative effect.

305 The structural equation models (SEM) showed that direct and indirect drivers
306 explained 70% (conditional R^2) of the variation in decomposition across the 18 forest
307 transects over 12 months (Table SM 8). Wood decomposition was directly influenced by
308 average temperature range (positive), average canopy openness (negative), termite
309 presence (positive), presence of both termites and fungi (negative) and wood density
310 (negative). Wood decomposition was indirectly influenced by factors that determine the
311 presence of termites and fungi, such as average canopy openness, average temperature
312 range and wood density (Fig. 5B).

313 4. Discussion

314 Our standardized decomposition experiment in eastern Amazon showed that wood
315 decomposition rates were most strongly determined by wood density. Although forest
316 disturbance class did not have additional direct controls on decomposition rates, the
317 structural equation model suggested that anthropogenic disturbance can influence wood

318 decomposition indirectly via shifts in forest structure that influence microclimate and the
319 indirect effect of microclimate on the presence of decomposers such as termites. These
320 findings highlight the complexity of the interrelations between biotic and abiotic factors
321 in the regulation of wood decomposition and the importance of considering both
322 structural and functional pathways through which disturbed forests alter carbon cycling
323 processes in tropical ecosystems.

324 4.1. *Wood density as a strong predictor of decomposition rates*

325 The inverse relationship (*e.g.* higher wood density corresponds to slower mass
326 loss) is well established in tropical forests (Chave et al., 2009; Mori et al., 2014) and was
327 clearly supported by our dataset. Importantly, this pattern remained consistent across all
328 forest classes, indicating that intrinsic wood properties were far more important than the
329 effects of forest disturbance (Fig. SM 4). The strong role of wood density is unsurprising
330 given the wide range of wood densities assessed ($0.36 - 1.15 \text{ g.cm}^{-3}$), which represents a
331 gradient from old growth species such as *Swartzia grandifolia* and *Handroanthus*
332 *serratifolius* which are all known for highly recalcitrant wood (Angyalossy-Alfonso and
333 Miller, 2002; Segoloni and Di Maria, 2018) to pioneer species like *Bixa arborea* and
334 *Jacaranda copaia* with woods containing more labile substrates (Reis et al., 2019).

335 Despite initial expectations, we found no evidence to support a “home field
336 advantage” (HFA). For example, more degraded forests did not show consistently faster
337 decomposition, despite being dominated by communities containing lower-density
338 species (Slik et al., 2008; Berenguer et al., 2018). The lack of a HFA suggests that
339 community composition and species turnover rates could be used to model deadwood
340 input and subsequent decomposition at scale. This is further supported by the same
341 inverse correlation with wood density found elsewhere in the biome (Aryal et al., 2022;
342 Chambers et al., 2000; Mori et al., 2014) and a global study showing that variation in

343 wood decomposition is mostly explained directly by wood characteristics, with half of
344 wood decomposition explained by its intrinsic characteristics and only a fifth by climatic
345 variables (Hu et al. 2018).

346 *4.2. Wood decomposition rates: temporal trends and species effects across forest*
347 *classes*

348 Although no direct effect of disturbance was detected, results suggest it influences
349 decomposition indirectly via changes in microclimate that affect decomposer activity.
350 Furthermore, it may be that there is a trade-off interaction between biotic and abiotic
351 factors that regulate decomposition. We demonstrated higher *max day* temperatures and
352 lower relative humidities in degraded forests compared to undisturbed forests (Table SM
353 7). In more degraded areas, although microclimatic conditions such as maximum
354 temperature, and greater decomposer attack (Senior et al., 2017) can theoretically
355 accelerate decomposition, lower relative humidity and greater temperature range can
356 counteract this effect, restricting certain decomposer species (Bradford et al., 2014; Gora
357 et al., 2019; Zhan et al., 2021). Despite this possibility, such processes would require
358 more studies to elucidate the factors that could mask differences in disturbance gradients.

359 *4.3. Wood decomposition of Amazonian species over time*

360 Decomposition increased progressively over the year, reflecting gradual structural
361 and chemical changes that facilitate colonization. The colonization of decomposers may
362 initially be slow due to physical and chemical barriers, such as high wood density,
363 compounds toxic to decomposers, or recalcitrant substrates (e.g., lignin) (Law et al., 2023;
364 Scharf, 2020). Over longer periods than the one year of our study, climatic conditions,
365 such as variations in humidity and temperature, could cause structural changes in the
366 wood, including microcracks, water absorption, and cycles of expansion and contraction,

367 making it gradually more vulnerable to the action of decomposers (Jankowska et al.,
368 2020).

369 Comparing our findings from other experiments, the values fell within the range
370 reported for other tropical forests (Law et al., 2019; Wijas et al., 2024), although
371 somewhat lower than values in Malaysia and Southeast Asia (Griffiths et al., 2020; Wu
372 et al., 2021). All these studies took place over one year, suggesting that study duration
373 alone does not explain the variation. Differences in decomposition rate of the same tree
374 species can emerge even in the same region with a similar climatic regime (Law et al.,
375 2019; Wijas et al., 2024), with changes in decomposer communities or microclimate
376 patterns affecting the path of decomposition (Gottschall et al., 2019; Wu et al., 2023).

377 *4.4. Termite activity as a strong driver of wood decomposition*

378 Overall, termites and fungi colonized approximately 33% and 52%, respectively,
379 of the dead wood among the forest classes by the end of the study, with highest
380 percentages after nine months of the experiment (Fig. SM 6), highlighting the
381 decomposition potential of these organisms (Aryal et al., 2022; Njoroge et al., 2025;
382 Seibold et al., 2021; Ulyshen, 2016). The presence of termites was strongly associated
383 with decomposition rates, and it was closely linked to the density of the wood, with lower
384 density blocks showing higher colonization frequencies corroborating previous studies
385 (Guo et al., 2021; Oberst et al., 2018). Dense plant species reduce foraging intensity,
386 possibly due to greater mechanical resistance, which can hinder both termites chewing
387 and the penetration of decomposing fungi (Liu et al., 2015; Oberst et al., 2018, Guo et al.,
388 2024). Notably, all wood blocks in our experiment were bark free. This may have
389 contributed to the strong role of termites as a recent global meta-analysis has shown that
390 wood without bark is often more readily colonized by wood-feeding termites, particularly

391 in tropical environments where these organisms are more abundant and active (Njoroge
392 et al., 2025).

393 *4.5. Microclimate and canopy openness as indirect pathways*

394 Microclimatic variation played a secondary but detectable role, with temperature
395 range and maximum daytime temperature affecting decomposition mainly after 12
396 months. This suggests that microclimate becomes more relevant at later stages, once
397 intrinsic barriers are weakened (Oberle et al., 2019). However, long-term experiments
398 would be needed to confirm or reject this possibility. Termite activity declined with wider
399 temperature ranges and *min night*, indicating that these ectothermic beings strongly
400 depend on thermal conditions to optimize their foraging activity (Wu et al., 2021).
401 Climatic seasonality in tropical forests, marked by wet and dry periods, also significantly
402 influences the population dynamics of these decomposers, as observed in our studies (Fig.
403 SM 5). Higher temperatures can stimulate termite activity (Zanne et al., 2022) but can
404 also reduce their efficiency in environments with high minimums (Wu et al., 2021), again
405 emphasizing the complexity of the interactions between microclimate and termite
406 decomposition. The stronger link between fungi and relative humidity reflects their
407 dependence on moist conditions (Gora et al., 2019). In addition, humidity close to the soil
408 may be more relevant to fungal activity than large-scale climatic conditions (Bradford et
409 al., 2014). However, these results on fungi only relate to their visible appearance of
410 fruiting bodies and visible hyphae, and more detailed assessments would be needed to
411 assess fungal activity (Charya, 2015).

412 **5. Conclusion**

413 We conducted a standardized experiment to examine the biotic and abiotic factors
414 that determine wood decomposition rates in modified Amazonian rainforests. Although

415 wood decomposition did not respond directly to forest disturbance classes, it is strongly
416 modulated by intrinsic wood characteristics, especially density. In addition, our results
417 provide some of the first evidence of indirect pathways, with changes in microclimate
418 resulting from forest disturbance influencing the role of decomposers. This demonstrates
419 that human-induced forest canopy openness may slow deadwood turnover by amplifying
420 temperature ranges that suppress decomposer activity, such as termite activity, a key on
421 decomposition. A longer-term and mechanistic understanding of these processes will help
422 improve our understanding of ecosystem processes in tropical forests facing high levels
423 of forest disturbance (Lapola et al. 2023) and temperature increases resulting from global
424 climate change (IPCC, 2023).

425 **Funding**

426 We are grateful for the following for financial support: Instituto Nacional de
427 Ciência e Tecnologia – Biodiversidade e Uso da Terra na Amazônia (CNPq 574008/2008-
428 0), the Conselho Nacional de Pesquisa (PELD-RAS CNPq, [441573/2020-7 and
429 445994/2024-0]), the Empresa Brasileira de Pesquisa Agropecuária – Embrapa (SEG:
430 02.08.06.005.00), the Coordenação de Aperfeiçoamento de Pessoal de Nível Superior –
431 Brasil (CAPES) – Finance Code 001, the Conselho Nacional de Pesquisa - CNPq
432 (140731/2021-0), the UK government Darwin Initiative (17-023), BNP Paribas
433 Foundation’s Climate and Biodiversity Initiative (Project Bioclimate), Natural
434 Environment Research Council (NERC) grants NE/F01614X/1, NE/G000816/1,
435 NE/K016431/1, NE/S01084X/1, NE/X015262/1 and NE/X019039/1.

436 **CRedit authorship contribution statement**

437 **Rodrigo O. do Nascimento:** Conceptualization, Methodology, Validation, Formal
438 analysis, Investigation, Data Curation, Writing – Original Draft, Visualization. **Erika**

439 **Berenguer:** Conceptualization, Methodology, Validation, Investigation, Writing –
440 Review & Editing, Funding acquisition. **Joice Ferreira:** Conceptualization,
441 Methodology, Validation, Writing – Review & Editing, Funding acquisition. **Carly**
442 **Stevens:** Validation, Writing – Review & Editing. **Marcos A. A. Filho:** Investigation,
443 Writing – Review & Editing. **Jos Barlow:** Conceptualization, Methodology, Validation,
444 Writing – Review & Editing, Supervision, Funding acquisition.

445 **Acknowledgments**

446 We thank the Large-Scale Biosphere–Atmosphere Program for logistical and
447 infrastructure support during field measurements. We are deeply grateful to all our field
448 and laboratory assistants, Josi, Xarope, Graveto e Bega. We also thank all collaborating
449 private landowners for their support and access to their land. We are also grateful to the
450 anonymous reviewers and the journal editors for their suggestions that helped improve
451 this manuscript. This is paper #127 of the Rede Amazônia Sustentável publication series.

452 **Declaration of competing interest**

453 The authors declare that they have no known competing financial interests or personal
454 relationships that could have influenced the work reported in this paper.

455 **References**

- 456 Alvares, C.A., Stape, J.L., Sentelhas, P.C., De Moraes Gonçalves, J.L., Sparovek, G.,
457 2013. Köppen’s climate classification map for Brazil. *metz* 22, 711–728.
458 <https://doi.org/10.1127/0941-2948/2013/0507>
- 459 Andrade, S., C, P., Corrêa, J., A, J., 2014. Estimativa do saldo de radiação instantâneo à
460 superfície para a cidade de Santarém-PA, através de imagens do Landsat 5-TM.

461 Rev. Bras. Geogr. Física 7, 653–661. <https://doi.org/10.26848/rbgf.v7.4.p653->
462 661

463 Angyalossy-Alfonso, V., Miller, R.B., 2002. Wood anatomy of the Brazilian species of
464 Swartzia and considerations within the tribe Swartzieae. IAWA Journal 23, 359–
465 390.

466 Aryal, D.R., De Jong, B.H.J., Gaona, S.O., Vega, J.M., Olguín, L.E., Cruz, S.L., 2022.
467 Fine Wood Decomposition Rates Decline with the Age of Tropical Successional
468 Forests in Southern Mexico: Implications to Ecosystem Carbon Storage.
469 Ecosystems 25, 661–677. <https://doi.org/10.1007/s10021-021-00678-w>

470 ASTM, 2008. Standard test methods for density and specific gravity (relative density)
471 of plastics by displacement. ASTM international.

472 Berenguer, E., Ferreira, J., Gardner, T.A., Aragão, L.E.O.C., De Camargo, P.B., Cerri,
473 C.E., Durigan, M., Oliveira Junior, R.C.D., Vieira, I.C.G., Barlow, J., 2014. A
474 large-scale field assessment of carbon stocks in human-modified tropical forests.
475 Global Change Biology 20, 3713–3726. <https://doi.org/10.1111/gcb.12627>

476 Berenguer, E., Lennox, G.D., Ferreira, J., Malhi, Y., Aragão, L.E.O.C., Barreto, J.R.,
477 Del Bon Espírito-Santo, F., Figueiredo, A.E.S., França, F., Gardner, T.A., Joly,
478 C.A., Palmeira, A.F., Quesada, C.A., Rossi, L.C., de Seixas, M.M.M., Smith,
479 C.C., Withey, K., Barlow, J., 2021. Tracking the impacts of El Niño drought and
480 fire in human-modified Amazonian forests. Proceedings of the National
481 Academy of Sciences 118, e2019377118.
482 <https://doi.org/10.1073/pnas.2019377118>

483 Berenguer, E., Malhi, Y., Brando, P., Cardoso Nunes Cordeiro, A., Ferreira, J., França,
484 F., Chesini Rossi, L., Maria Moraes de Seixas, M., Barlow, J., 2018. Tree
485 growth and stem carbon accumulation in human-modified Amazonian forests

486 following drought and fire. *Philosophical Transactions of the Royal Society B:*
487 *Biological Sciences* 373, 20170308. <https://doi.org/10.1098/rstb.2017.0308>

488 Bradford, M.A., Maynard, D.S., Crowther, T.W., Frankson, P.T., Mohan, J.E.,
489 Steinrueck, C., Veen, G.F. (Ciska), King, J.R., Warren II, R.J., 2021.
490 Belowground community turnover accelerates the decomposition of standing
491 dead wood. *Ecology* 102, e03484. <https://doi.org/10.1002/ecy.3484>

492 Bradford, M.A., Warren II, R.J., Baldrian, P., Crowther, T.W., Maynard, D.S., Oldfield,
493 E.E., Wieder, W.R., Wood, S.A., King, J.R., 2014. Climate fails to predict wood
494 decomposition at regional scales. *Nature Clim Change* 4, 625–630.
495 <https://doi.org/10.1038/nclimate2251>

496 Brooks, M., Kristensen, K., Benthem, K. van, Magnusson, A., Berg, C., Nielsen, A.,
497 Skaug, H., Mächler, M., Bolker, B., 2017. glmmTMB Balances Speed and
498 Flexibility Among Packages for Zero-inflated Generalized Linear Mixed
499 Modeling. *The R Journal*.

500 Bullock, E.L., Woodcock, C.E., Souza Jr., C., Olofsson, P., 2020. Satellite-based
501 estimates reveal widespread forest degradation in the Amazon. *Global Change*
502 *Biology* 26, 2956–2969. <https://doi.org/10.1111/gcb.15029>

503 Chambers, J.Q., Higuchi, N., Schimel, J.P., Ferreira, L.V., Melack, J.M., 2000.
504 Decomposition and carbon cycling of dead trees in tropical forests of the central
505 Amazon. *Oecologia* 122, 380–388. <https://doi.org/10.1007/s004420050044>

506 Charya, M.A., 2015. Fungi: An Overview, in: Bahadur, B., Venkat Rajam, M.,
507 Sahijram, L., Krishnamurthy, K.V. (Eds.), *Plant Biology and Biotechnology:*
508 *Volume I: Plant Diversity, Organization, Function and Improvement*. Springer
509 India, New Delhi, pp. 197–215. https://doi.org/10.1007/978-81-322-2286-6_7

510 Chave, J., Coomes, D., Jansen, S., Lewis, S.L., Swenson, N.G., Zanne, A.E., 2009.
511 Towards a worldwide wood economics spectrum. *Ecology Letters* 12, 351–366.
512 <https://doi.org/10.1111/j.1461-0248.2009.01285.x>

513 Dambros, C.S., Morais, J.W., Vasconcellos, A., Franklin, E., 2020. Defining a termite
514 sampling protocol for ecological studies: An effective method to increase
515 statistical power. *European Journal of Soil Biology* 96, 103145.
516 <https://doi.org/10.1016/j.ejsobi.2019.103145>

517 Dawson, S.K., Boddy, L., Halbwachs, H., Bässler, C., Andrew, C., Crowther, T.W.,
518 Heilmann-Clausen, J., Nordén, J., Ovaskainen, O., Jönsson, M., 2019. Handbook
519 for the measurement of macrofungal functional traits: A start with basidiomycete
520 wood fungi. *Functional Ecology* 33, 372–387. [https://doi.org/10.1111/1365-](https://doi.org/10.1111/1365-2435.13239)
521 [2435.13239](https://doi.org/10.1111/1365-2435.13239)

522 Dossa, G.G.O., Paudel, E., Schaefer, D., Zhang, J.-L., Cao, K.-F., Xu, J.-C., Harrison,
523 R.D., 2020. Quantifying the factors affecting wood decomposition across a
524 tropical forest disturbance gradient. *Forest Ecology and Management* 468,
525 118166. <https://doi.org/10.1016/j.foreco.2020.118166>

526 Duffy, P.B., Brando, P., Asner, G.P., Field, C.B., 2015. Projections of future
527 meteorological drought and wet periods in the Amazon. *Proceedings of the*
528 *National Academy of Sciences* 112, 13172–13177.
529 <https://doi.org/10.1073/pnas.1421010112>

530 Ewers, R.M., Boyle, M.J.W., Gleave, R.A., Plowman, N.S., Benedick, S., Bernard, H.,
531 Bishop, T.R., Bakhtiar, E.Y., Chey, V.K., Chung, A.Y.C., Davies, R.G.,
532 Edwards, D.P., Eggleton, P., Fayle, T.M., Hardwick, S.R., Homathevi, R.,
533 Kitching, R.L., Khoo, M.S., Luke, S.H., March, J.J., Nilus, R., Pfeifer, M., Rao,
534 S.V., Sharp, A.C., Snaddon, J.L., Stork, N.E., Struebig, M.J., Wearn, O.R.,

535 Yusah, K.M., Turner, E.C., 2015. Logging cuts the functional importance of
536 invertebrates in tropical rainforest. *Nat Commun* 6, 6836.
537 <https://doi.org/10.1038/ncomms7836>

538 Fearnside, P.M., 1997. Wood density for estimating forest biomass in Brazilian
539 Amazonia. *Forest Ecology and Management* 90, 59–87.
540 [https://doi.org/10.1016/S0378-1127\(96\)03840-6](https://doi.org/10.1016/S0378-1127(96)03840-6)

541 Fonseca, M.G., Alves, L.M., Aguiar, A.P.D., Arai, E., Anderson, L.O., Rosan, T.M.,
542 Shimabukuro, Y.E., de Aragão, L.E.O. e C., 2019. Effects of climate and land-
543 use change scenarios on fire probability during the 21st century in the Brazilian
544 Amazon. *Global Change Biology* 25, 2931–2946.
545 <https://doi.org/10.1111/gcb.14709>

546 Gardner, T.A., Ferreira, J., Barlow, J., Lees, A.C., Parry, L., Vieira, I.C.G., Berenguer,
547 E., Abramovay, R., Aleixo, A., Andretti, C., Aragão, L.E.O.C., Araújo, I., de
548 Ávila, W.S., Bardgett, R.D., Batistella, M., Begotti, R.A., Beldini, T., de Blas,
549 D.E., Braga, R.F., Braga, D. de L., de Brito, J.G., de Camargo, P.B., Campos
550 dos Santos, F., de Oliveira, V.C., Cordeiro, A.C.N., Cardoso, T.M., de Carvalho,
551 D.R., Castelani, S.A., Chaul, J.C.M., Cerri, C.E., Costa, F. de A., da Costa,
552 C.D.F., Coudel, E., Coutinho, A.C., Cunha, D., D'Antona, Á., Dezincourt, J.,
553 Dias-Silva, K., Durigan, M., Esquerdo, J.C.D.M., Feres, J., Ferraz, S.F. de B.,
554 Ferreira, A.E. de M., Fiorini, A.C., da Silva, L.V.F., Frazão, F.S., Garrett, R.,
555 Gomes, A. dos S., Gonçalves, K. da S., Guerrero, J.B., Hamada, N., Hughes,
556 R.M., Iglioni, D.C., Jesus, E. da C., Juen, L., Junior, M., Junior, J.M.B. de O.,
557 Junior, R.C. de O., Junior, C.S., Kaufmann, P., Korasaki, V., Leal, C.G., Leitão,
558 R., Lima, N., Almeida, M. de F.L., Lourival, R., Louzada, J., Nally, R.M.,
559 Marchand, S., Maués, M.M., Moreira, F.M.S., Morsello, C., Moura, N.,

560 Nessimian, J., Nunes, S., Oliveira, V.H.F., Pardini, R., Pereira, H.C., Pompeu,
561 P.S., Ribas, C.R., Rossetti, F., Schmidt, F.A., da Silva, R., da Silva, R.C.V.M.,
562 da Silva, T.F.M.R., Silveira, J., Siqueira, J.V., de Carvalho, T.S., Solar, R.R.C.,
563 Tancredi, N.S.H., Thomson, J.R., Torres, P.C., Vaz-de-Mello, F.Z., Veiga,
564 R.C.S., Venturieri, A., Viana, C., Weinhold, D., Zanetti, R., Zuanon, J., 2013. A
565 social and ecological assessment of tropical land uses at multiple scales: the
566 Sustainable Amazon Network. *Philosophical Transactions of the Royal Society*
567 *B: Biological Sciences* 368, 20120166. <https://doi.org/10.1098/rstb.2012.0166>

568 Giardina, C.P., 2019. Advancing Our Understanding of Woody Debris in Tropical
569 Forests. *Ecosystems* 22, 1173–1175. <https://doi.org/10.1007/s10021-019-00381->
570 x

571 Gonsamo, A., D’odorico, P., Pellikka, P., 2013. Measuring fractional forest canopy
572 element cover and openness—definitions and methodologies revisited. *Oikos*
573 122, 1283–1291. <https://doi.org/10.1111/j.1600-0706.2013.00369.x>

574 Gora, E.M., Kneale, R.C., Larjavaara, M., Muller-Landau, H.C., 2019. Dead Wood
575 Necromass in a Moist Tropical Forest: Stocks, Fluxes, and Spatiotemporal
576 Variability. *Ecosystems* 22, 1189–1205. <https://doi.org/10.1007/s10021-019->
577 00341-5

578 Gottschall, F., Davids, S., Newiger-Dous, T.E., Auge, H., Cesarz, S., Eisenhauer, N.,
579 2019. Tree species identity determines wood decomposition via microclimatic
580 effects. *Ecology and Evolution* 9, 12113–12127.
581 <https://doi.org/10.1002/ece3.5665>

582 Grace, J.B., Schoolmaster Jr, D.R., Guntenspergen, G.R., Little, A.M., Mitchell, B.R.,
583 Miller, K.M., Schweiger, E.W., 2012. Guidelines for a graph-theoretic

584 implementation of structural equation modeling. *Ecosphere* 3, 1–44.
585 <https://doi.org/10.1890/ES12-00048.1>

586 Griffiths, H.M., Ashton, L.A., Parr, C.L., Eggleton, P., 2021. The impact of invertebrate
587 decomposers on plants and soil. *New Phytologist* 231, 2142–2149.
588 <https://doi.org/10.1111/nph.17553>

589 Griffiths, H.M., Eggleton, P., Hemming-Schroeder, N., Swinfield, T., Woon, J.S.,
590 Allison, S.D., Coomes, D.A., Ashton, L.A., Parr, C.L., 2020. Carbon flux and
591 forest dynamics: Increased deadwood decomposition in tropical rainforest tree-
592 fall canopy gaps. *Global Change Biology* 27, 1601–1613.
593 <https://doi.org/10.1111/gcb.15488>

594 Guo, C., Tuo, B., Ci, H., Yan, E.-R., Cornelissen, J.H.C., 2021. Dynamic feedbacks
595 among tree functional traits, termite populations and deadwood turnover. *Journal*
596 *of Ecology* 109, 1578–1590. <https://doi.org/10.1111/1365-2745.13604>

597 Guo, C., Tuo, B., Seibold, S., Ci, H., Sai, B.-L., Qin, H.-T., Yan, E.-R., Cornelissen,
598 J.H.C., 2024. Seasonally Changing Interactions of Species Traits of Termites
599 and Trees Promote Complementarity in Coarse Wood Decomposition. *Ecology*
600 *Letters* 27, e70002. <https://doi.org/10.1111/ele.70002>

601 Hardwick, S.R., Toumi, R., Pfeifer, M., Turner, E.C., Nilus, R., Ewers, R.M., 2015. The
602 relationship between leaf area index and microclimate in tropical forest and oil
603 palm plantation: Forest disturbance drives changes in microclimate. *Agricultural*
604 *and Forest Meteorology* 201, 187–195.
605 <https://doi.org/10.1016/j.agrformet.2014.11.010>

606 Harmon, M.E., Fasth, B.G., Yatskov, M., Kastendick, D., Rock, J., Woodall, C.W.,
607 2020. Release of coarse woody detritus-related carbon: a synthesis across forest

608 biomes. *Carbon Balance Manage* 15, 1. [https://doi.org/10.1186/s13021-019-](https://doi.org/10.1186/s13021-019-0136-6)
609 0136-6

610 Harmon, M.E., Franklin, J.F., Swanson, F.J., Sollins, P., Gregory, S.V., Lattin, J.D.,
611 Anderson, N.H., Cline, S.P., Aumen, N.G., Sedell, J.R., Lienkaemper, G.W.,
612 Cromack, K., Cummins, K.W., 1986. Ecology of Coarse Woody Debris in
613 Temperate Ecosystems, in: MacFadyen, A., Ford, E.D. (Eds.), *Advances in*
614 *Ecological Research*. Academic Press, pp. 133–302.
615 [https://doi.org/10.1016/S0065-2504\(08\)60121-X](https://doi.org/10.1016/S0065-2504(08)60121-X)

616 Hartig, F., 2016. DHARMA: Residual Diagnostics for Hierarchical (Multi-Level /
617 Mixed) Regression Models. CRAN: Contributed Packages.
618 <https://doi.org/10.32614/cran.package.dharma>

619 Hu, Z., Michaletz, S.T., Johnson, D.J., McDowell, N.G., Huang, Z., Zhou, X., Xu, C.,
620 2018. Traits drive global wood decomposition rates more than climate. *Global*
621 *Change Biology* 24, 5259–5269. <https://doi.org/10.1111/gcb.14357>

622 INMET. Instituto Nacional de Pesquisas Espaciais. Coordenação-geral de ciências da
623 terra. Programa de monitoramento dos biomas brasileiros. DETER –
624 Monitoramento Diário da Supressão e Degradação da Vegetação Nativa –
625 Alertas – Amazônia/Cerrado/Pantanal.
626 <https://terrabrasilis.dpi.inpe.br/downloads/> (accessed 10 January 2025).

627 IPCC, 2023: *Climate Change 2023: Synthesis Report*. Contribution of Working Groups
628 I, II and III to the Sixth Assessment Report of the Intergovernmental Panel on
629 Climate Change [Core Writing Team, H. Lee and J. Romero (eds.)]. IPCC,
630 Geneva, Switzerland, pp. 35-115, doi: 10.59327/IPCC/AR6-9789291691647.

631 Irbe, I., Karadelev, M., Andersons, B., 2010. Qualitative-quantitative analysis of wood-
632 inhabiting fungi in external wooden structures of the Latvian cultural heritage.

633 Jankowska, A., Rybak, K., Nowacka, M., Boruszewski, P., 2020. Insight of Weathering
634 Processes Based on Monitoring Surface Characteristic of Tropical Wood
635 Species. *Coatings* 10, 877. <https://doi.org/10.3390/coatings10090877>

636 Jucker, T., Hardwick, S.R., Both, S., Elias, D.M.O., Ewers, R.M., Milodowski, D.T.,
637 Swinfield, T., Coomes, D.A., 2018. Canopy structure and topography jointly
638 constrain the microclimate of human-modified tropical landscapes. *Global*
639 *Change Biology* 24, 5243–5258. <https://doi.org/10.1111/gcb.14415>

640 Lapola, D.M., Pinho, P., Barlow, J., Aragão, L.E., Berenguer, E., Carmenta, R., Liddy,
641 H.M., Seixas, H., Silva, C.V., Silva-Junior, C.H., Alencar, A.A.C., Anderson,
642 L.O., Armenteras, D., Brovkin, V., Calders, K., Chambers, J., Chini, L., Costa,
643 M.H., Faria, B.L., Fearnside, P.M., Ferreira, J., Gatti, L., Gutierrez-Velez, V.H.,
644 Han, Z., Hibbard, K., Koven, C., Lawrence, P., Pongratz, J., Portela, B.T.T.,
645 Rounsevell, M., Ruane, A.C., Schaldach, R., da Silva, S.S., von Randow, C.,
646 Walker, W.S., 2023. The drivers and impacts of Amazon forest degradation.
647 *Science* 379, eabp8622. <https://doi.org/10.1126/science.abp8622>

648 Law, S., Eggleton, P., Griffiths, H., Ashton, L., Parr, C., 2019. Suspended Dead Wood
649 Decomposes Slowly in the Tropics, with Microbial Decay Greater than Termite
650 Decay. *Ecosystems* 22, 1176–1188. <https://doi.org/10.1007/s10021-018-0331-4>

651 Law, S., Flores-Moreno, H., Cheesman, A.W., Clement, R., Rosenfield, M., Yatsko, A.,
652 Cernusak, L.A., Dalling, J.W., Canam, T., Iqsaysa, I.A., Duan, E.S., Allison,
653 S.D., Eggleton, P., Zanne, A.E., 2023. Wood traits explain microbial but not
654 termite-driven decay in Australian tropical rainforest and savanna. *Journal of*
655 *Ecology* 111, 982–993. <https://doi.org/10.1111/1365-2745.14090>

656 Lefcheck, J.S., 2016. piecewiseSEM: Piecewise structural equation modelling in r for
657 ecology, evolution, and systematics. *Methods in Ecology and Evolution* 7, 573–
658 579. <https://doi.org/10.1111/2041-210X.12512>

659 Liu, G., Cornwell, W.K., Cao, K., Hu, Y., Van Logtestijn, R.S.P., Yang, S., Xie, X.,
660 Zhang, Y., Ye, D., Pan, X., Ye, X., Huang, Z., Dong, M., Cornelissen, J.H.C.,
661 2015. Termites amplify the effects of wood traits on decomposition rates among
662 multiple bamboo and dicot woody species. *Journal of Ecology* 103, 1214–1223.
663 <https://doi.org/10.1111/1365-2745.12427>

664 Lüdecke, D., 2013. sjPlot: Data Visualization for Statistics in Social Science.
665 <https://doi.org/10.32614/CRAN.package.sjPlot>

666 Marsh, C.D., Hill, R.A., Nowak, M.G., Hankinson, E., Abdullah, A., Gillingham, P.,
667 Korstjens, A.H., 2022. Measuring and modelling microclimatic air temperature
668 in a historically degraded tropical forest. *Int J Biometeorol* 66, 1283–1295.
669 <https://doi.org/10.1007/s00484-022-02276-4>

670 Martin, A.R., Domke, G.M., Doraisami, M., Thomas, S.C., 2021. Carbon fractions in
671 the world's dead wood. *Nat Commun* 12, 889. [https://doi.org/10.1038/s41467-](https://doi.org/10.1038/s41467-021-21149-9)
672 [021-21149-9](https://doi.org/10.1038/s41467-021-21149-9)

673 Mori, S., Itoh, A., Nanami, S., Tan, S., Chong, L., Yamakura, T., 2014. Effect of wood
674 density and water permeability on wood decomposition rates of 32 Bornean
675 rainforest trees. *Journal of Plant Ecology* 7, 356–363.
676 <https://doi.org/10.1093/jpe/rtt041>

677 Njoroge, D.M., Dossa, G.G.O., Schaefer, D., Zuo, J., Ulyshen, M.D., Seibold, S.,
678 Zanne, A.E., Oberle, B., Harrison, R.D., Liu, S., Li, X., Birkemoe, T., Taylor,
679 M.K., Burton, P.J., Lindenmayer, D.B., Kouki, J., Adhikari, Y., Cornelissen,

680 J.H.C., 2025. The effects of invertebrates on wood decomposition across the
681 world. *Biological Reviews* 100, 158–171. <https://doi.org/10.1111/brv.13134>

682 Nogueira, E.M., Nelson, B.W., Fearnside, P.M., 2005. Wood density in dense forest in
683 central Amazonia, Brazil. *Forest Ecology and Management* 208, 261–286.
684 <https://doi.org/10.1016/j.foreco.2004.12.007>

685 Oberle, B., Lee, M.R., Myers, J.A., Osazuwa-Peters, O.L., Spasojevic, M.J., Walton,
686 M.L., Young, D.F., Zanne, A.E., 2019. Accurate forest projections require long-
687 term wood decay experiments because plant trait effects change through time.
688 *Ecology* 100, 2, 864-875. <https://doi.org/10.1111/gcb.14873>

689 Oberst, S., Lai, J.C.S., Evans, T.A., 2018. Key physical wood properties in termite
690 foraging decisions. *Journal of The Royal Society Interface* 15, 20180505.
691 <https://doi.org/10.1098/rsif.2018.0505>

692 Palace, M., Keller, M., Silva, H., 2008. Necromass production: studies in undisturbed
693 and logged Amazon forests. *Ecological Applications* 18, 873–884.
694 <https://doi.org/10.1890/06-2022.1>

695 Pan, Y., Birdsey, R.A., Fang, J., Houghton, R., Kauppi, P.E., Kurz, W.A., Phillips,
696 O.L., Shvidenko, A., Lewis, S.L., Canadell, J.G., Ciais, P., Jackson, R.B.,
697 Pacala, S.W., McGuire, A.D., Piao, S., Rautiainen, A., Sitch, S., Hayes, D.,
698 2011. A Large and Persistent Carbon Sink in the World’s Forests. *Science* 333,
699 988–993. <https://doi.org/10.1126/science.1201609>

700 Pinho, B.X., Melo, F.P.L., ter Braak, C.J.F., Bauman, D., Maréchaux, I., Tabarelli, M.,
701 Benchimol, M., Arroyo-Rodriguez, V., Santos, B.A., Hawes, J.E., Berenguer,
702 E., Ferreira, J., Silveira, J.M., Peres, C.A., Rocha-Santos, L., Souza, F.C.,
703 Gonçalves-Souza, T., Mariano-Neto, E., Faria, D., Barlow, J., 2024. Winner–

704 loser plant trait replacements in human-modified tropical forests. *Nat Ecol Evol*
705 9, 282–295. <https://doi.org/10.1038/s41559-024-02592-5>

706 R Core Team, 2024. *R: A Language and Environment for Statistical Computing*. R
707 Foundation for Statistical Computing, Vienna, Austria.

708 Reis, P.C.M.D.R., Souza, A.L.D., Reis, L.P., Carvalho, A.M.M.L., Mazzei, L., Reis,
709 A.R.S., Torres, C.M.M.E., 2019. Agrupamento de espécies madeireiras da
710 Amazônia com base em propriedades físicas e mecânicas. *Ciênc. Florest.* 29,
711 336–346. <https://doi.org/10.5902/1980509828114>

712 Restrepo-Coupe, N., da Rocha, H.R., Hutyrá, L.R., da Araujo, A.C., Borma, L.S.,
713 Christoffersen, B., Cabral, O.M.R., de Camargo, P.B., Cardoso, F.L., da Costa,
714 A.C.L., Fitzjarrald, D.R., Goulden, M.L., Kruijt, B., Maia, J.M.F., Malhi, Y.S.,
715 Manzi, A.O., Miller, S.D., Nobre, A.D., von Randow, C., Sá, L.D.A., Sakai,
716 R.K., Tota, J., Wofsy, S.C., Zanchi, F.B., Saleska, S.R., 2013. What drives the
717 seasonality of photosynthesis across the Amazon basin? A cross-site analysis of
718 eddy flux tower measurements from the Brasil flux network. *Agricultural and*
719 *Forest Meteorology* 182–183, 128–144.
720 <https://doi.org/10.1016/j.agrformet.2013.04.031>

721 Risch, A.C., Page-Dumroese, D.S., Schweiger, A.K., Beattie, J.R., Curran, M.P., Finér,
722 L., Hyslop, M.D., Liu, Y., Schütz, M., Terry, T.A., Wang, W., Jurgensen, M.F.,
723 2022. Controls of Initial Wood Decomposition on and in Forest Soils Using
724 Standard Material. *Front. For. Glob. Change* 5.
725 <https://doi.org/10.3389/ffgc.2022.829810>

726 Russell, M.B., Fraver, S., Aakala, T., Gove, J.H., Woodall, C.W., D’Amato, A.W.,
727 Ducey, M.J., 2015. Quantifying carbon stores and decomposition in dead wood:

728 A review. *Forest Ecology and Management* 350, 107–128.
729 <https://doi.org/10.1016/j.foreco.2015.04.033>

730 Scharf, M.E., 2020. Challenges and physiological implications of wood feeding in
731 termites. *Current Opinion in Insect Science, Global change biology * Molecular*
732 *physiology* section 41, 79–85. <https://doi.org/10.1016/j.cois.2020.07.007>

733 Schleppei, P., Conedera, M., Sedivy, I., Thimonier, A., 2007. Correcting non-linearity
734 and slope effects in the estimation of the leaf area index of forests from
735 hemispherical photographs. *Agricultural and Forest Meteorology* 144, 236–242.
736 <https://doi.org/10.1016/j.agrformet.2007.02.004>

737 Seibold, S., Rammer, W., Hothorn, T., Seidl, R., Ulyshen, M.D., Lorz, J., Cadotte,
738 M.W., Lindenmayer, D.B., Adhikari, Y.P., Aragón, R., Bae, S., Baldrian, P.,
739 Barimani Varandi, H., Barlow, J., Bässler, C., Beauchêne, J., Berenguer, E.,
740 Bergamin, R.S., Birkemoe, T., Boros, G., Brandl, R., Brustel, H., Burton, P.J.,
741 Cakpo-Tossou, Y.T., Castro, J., Cateau, E., Cobb, T.P., Farwig, N., Fernández,
742 R.D., Firn, J., Gan, K.S., González, G., Gossner, M.M., Habel, J.C., Hébert, C.,
743 Heibl, C., Heikkala, O., Hemp, A., Hemp, C., Hjältén, J., Hotes, S., Kouki, J.,
744 Lachat, T., Liu, J., Liu, Y., Luo, Y.-H., Macandog, D.M., Martina, P.E., Mukul,
745 S.A., Nachin, B., Nisbet, K., O'Halloran, J., Oxbrough, A., Pandey, J.N.,
746 Pavlíček, T., Pawson, S.M., Rakotondranary, J.S., Ramanamanjato, J.-B., Rossi,
747 L., Schmidl, J., Schulze, M., Seaton, S., Stone, M.J., Stork, N.E., Suran, B.,
748 Sverdrup-Thygeson, A., Thorn, S., Thyagarajan, G., Wardlaw, T.J., Weisser,
749 W.W., Yoon, S., Zhang, N., Müller, J., 2021. The contribution of insects to
750 global forest deadwood decomposition. *Nature* 597, 77–81.
751 <https://doi.org/10.1038/s41586-021-03740-8>

752 Segoloni, E., Di Maria, F., 2018. UV–VIS spectral and GC–MS characterization of
753 *Handroanthus serratifolius* (Vahl.) Grose (a.k.a. *Tabebuia serratifolia* (Vahl.)
754 Nichols/Lapacho) heartwood main extractives: a comparison of protocols aimed
755 at a practical evaluation of Lapachol and Dehydro- α -Lapachone content. *Eur. J.*
756 *Wood Prod.* 76, 1547–1561. <https://doi.org/10.1007/s00107-018-1331-y>

757 Senior, R.A., Hill, J.K., Benedick, S., Edwards, D.P., 2017. Tropical forests are
758 thermally buffered despite intensive selective logging. *Global Change Biology*
759 24, 1267–1278. <https://doi.org/10.1111/gcb.13914>

760 Shipley, B., 2013. The AIC model selection method applied to path analytic models
761 compared using ad-separation test. *Ecology* 94, 560–564.
762 <https://doi.org/10.1890/12-0976.1>

763 Slik, J.W.F., Bernard, C.S., Breman, F.C., Van Beek, M., Salim, A., Sheil, D., 2008.
764 Wood Density as a Conservation Tool: Quantification of Disturbance and
765 Identification of Conservation-Priority Areas in Tropical Forests. *Conservation*
766 *Biology* 22, 1299–1308. <https://doi.org/10.1111/j.1523-1739.2008.00986.x>

767 Townsend, A.R., Cleveland, C.C., Houlton, B.Z., Alden, C.B., White, J.W., 2011.
768 Multi-element regulation of the tropical forest carbon cycle. *Frontiers in*
769 *Ecology and the Environment* 9, 9–17. <https://doi.org/10.1890/100047>

770 Ulyshen, M.D., 2016. Wood decomposition as influenced by invertebrates. *Biological*
771 *Reviews* 91, 70–85. <https://doi.org/10.1111/brv.12158>

772 Wijas, B.J., Flores-Moreno, H., Allison, S.D., Rodriguez, L.C., Cheesman, A.W.,
773 Cernusak, L.A., Clement, R., Cornwell, W.K., Duan, E.S., Eggleton, P.,
774 Rosenfield, M.V., Yatsko, A.R., Zanne, A.E., 2024. Drivers of wood decay in
775 tropical ecosystems: Termites versus microbes along spatial, temporal and

776 experimental precipitation gradients. *Functional Ecology* 38, 546–559.
777 <https://doi.org/10.1111/1365-2435.14494>

778 Wu, D., Staab, M., Yu, M., 2021. Canopy Closure Retards Fine Wood Decomposition
779 in Subtropical Regenerating Forests. *Ecosystems* 24, 1875–1890.
780 <https://doi.org/10.1007/s10021-021-00622-y>

781 Wu, C., Yuan, X., Yang, G., Ning, D., Zhang, Y., Liu, Y., Wang, G.G., 2024. How does
782 position affect the decomposition of fine woody debris in subtropical forest?
783 *Forest Ecology and Management* 560, 121829.
784 <https://doi.org/10.1016/j.foreco.2024.121829>

785 Wu, D., Seibold, S., Pietsch, K.A., Ellwood, M.D.F., Yu, M., 2023. Tree species
786 richness increases spatial variation but not overall wood decomposition. *Soil*
787 *Biology and Biochemistry* 183, 109060.
788 <https://doi.org/10.1016/j.soilbio.2023.109060>

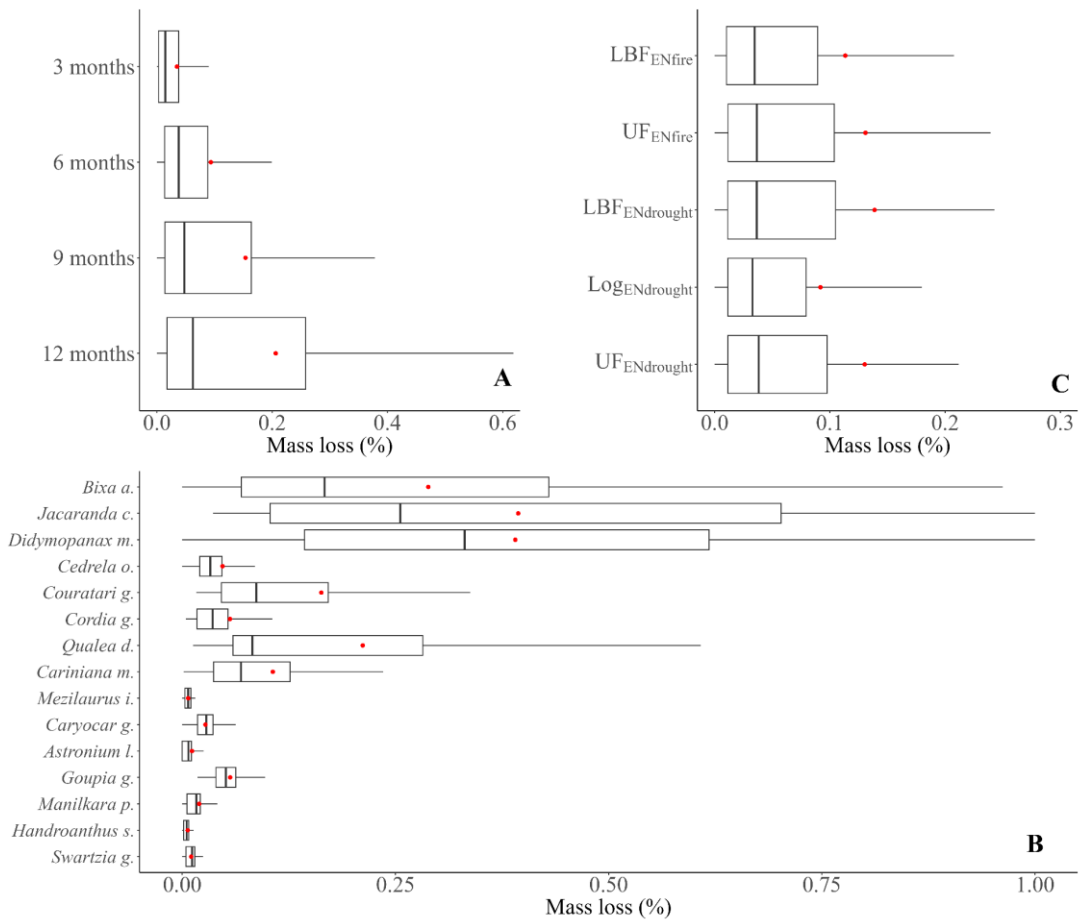
789 Zanne, A.E., Flores-Moreno, H., Powell, J.R., Cornwell, W.K., Dalling, J.W., Austin,
790 A.T., Classen, A.T., Eggleton, P., Okada, K., Parr, C.L., Adair, E.C., Adu-
791 Bredu, S., Alam, M.A., Alvarez-Garzón, C., Apgaua, D., Aragón, R., Ardon, M.,
792 Arndt, S.K., Ashton, L.A., Barber, N.A., Beauchêne, J., Berg, M.P., Beringer, J.,
793 Boer, M.M., Bonet, J.A., Bunney, K., Burkhardt, T.J., Carvalho, D., Castillo-
794 Figueroa, D., Cernusak, L.A., Cheesman, A.W., Cirne-Silva, T.M., Cleverly,
795 J.R., Cornelissen, J.H.C., Curran, T.J., D’Angioli, A.M., Dallstream, C.,
796 Eisenhauer, N., Evouna Ondo, F., Fajardo, A., Fernandez, R.D., Ferrer, A.,
797 Fontes, M.A.L., Galatowitsch, M.L., González, G., Gottschall, F., Grace, P.R.,
798 Granda, E., Griffiths, H.M., Guerra Lara, M., Hasegawa, M., Hefting, M.M.,
799 Hinko-Najera, N., Hutley, L.B., Jones, J., Kahl, A., Karan, M., Keuskamp, J.A.,
800 Lardner, T., Liddell, M., Macfarlane, C., Macinnis-Ng, C., Mariano, R.F.,

801 Méndez, M.S., Meyer, W.S., Mori, A.S., Moura, A.S., Northwood, M., Ogaya,
802 R., Oliveira, R.S., Orgiazzi, A., Pardo, J., Peguero, G., Penuelas, J., Perez, L.I.,
803 Posada, J.M., Prada, C.M., Přívětivý, T., Prober, S.M., Prunier, J., Quansah,
804 G.W., Resco de Dios, V., Richter, R., Robertson, M.P., Rocha, L.F., Rúa, M.A.,
805 Sarmiento, C., Silberstein, R.P., Silva, M.C., Siqueira, F.F., Stillwagon, M.G.,
806 Stol, J., Taylor, M.K., Teste, F.P., Tng, D.Y.P., Tucker, D., Türke, M., Ulyshen,
807 M.D., Valverde-Barrantes, O.J., van den Berg, E., van Logtestijn, R.S.P., Veen,
808 G.F. (Ciska), Vogel, J.G., Wardlaw, T.J., Wiehl, G., Wirth, C., Woods, M.J.,
809 Zalamea, P.-C., 2022. Termite sensitivity to temperature affects global wood
810 decay rates. *Science* 377, 1440–1444. <https://doi.org/10.1126/science.abo3856>
811 Zanne, A.E., Lopez-Gonzalez, G., Coomes, D.A., Ilic, J., Jansen, S., Lewis, S.L.,
812 Miller, R.B., Swenson, N.G., Wiemann, M.C., Chave, J., 2009. Global wood
813 density database. *Dryad*. <https://doi.org/10.5061/dryad.234>
814 Zhan, Z., Meiling, X., Li, Y., Dong, M., 2021. The relationship between fungal growth
815 rate and temperature and humidity. *International Journal of Engineering and*
816 *Management Research* 11, 78–83. <http://dx.doi.org/10.31033/ijemr.11.3.13>
817
818
819
820
821
822
823
824
825



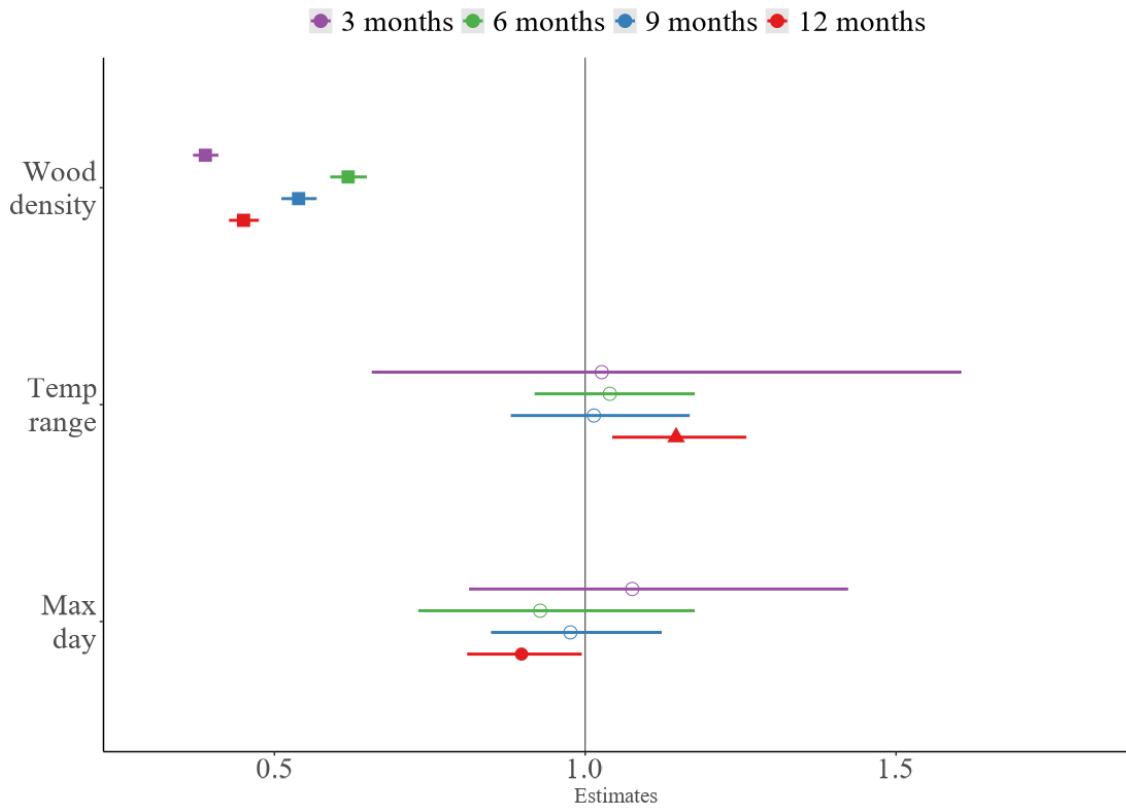
827

828 Fig. 1. Experimental sampling design. In each of the 18 sampled transects, we established three
 829 sampling points, located at 0, 150 and 300 m. In each sampling point we installed four collars
 830 (brown squares) and a microclimate data logger, which registered both temperature and relative
 831 humidity (blue square). Hemispherical photographs were taken monthly at each sample point to
 832 quantify canopy openness (green squares).



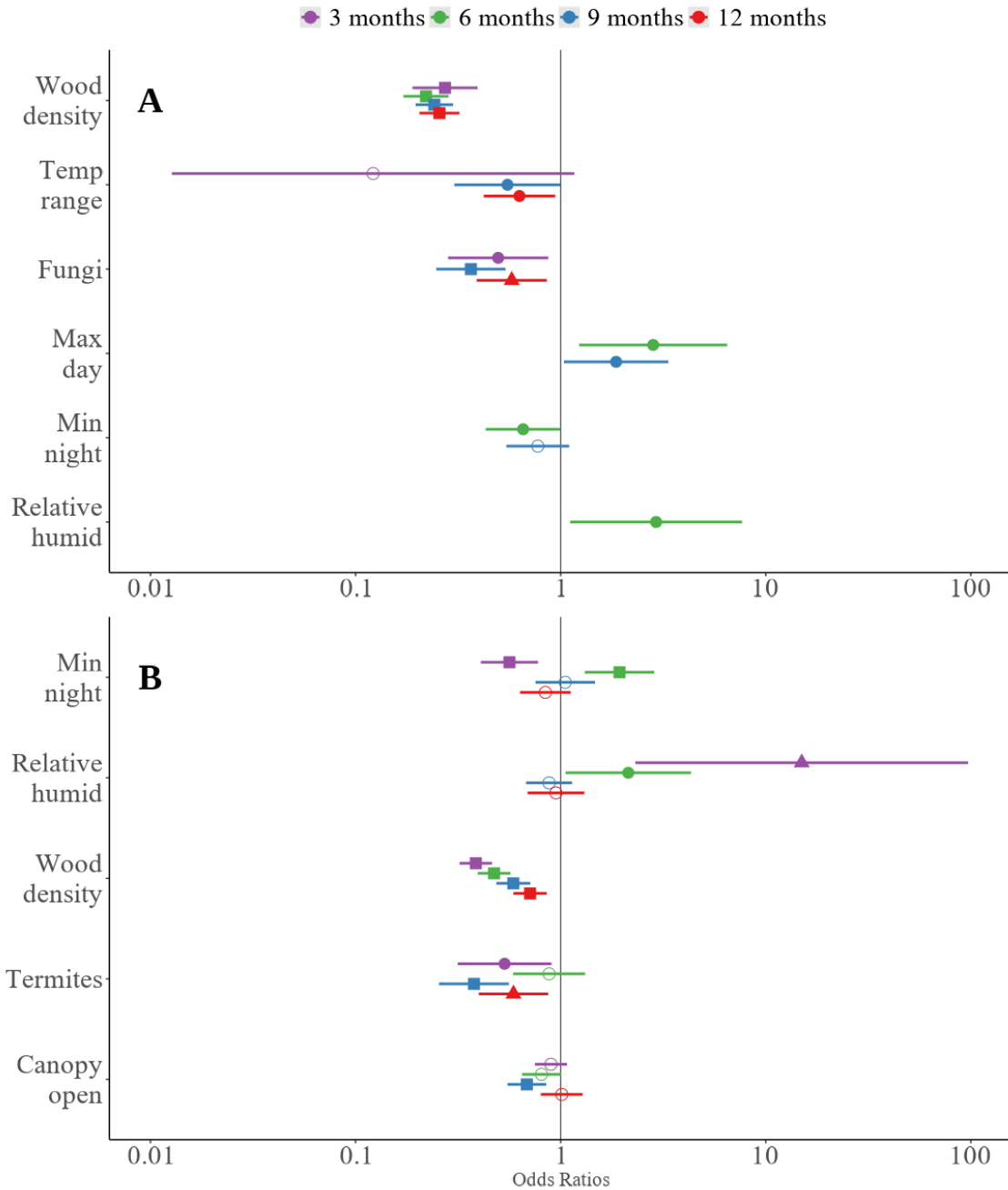
833

834 Fig. 2. Proportional mass loss of wood blocks across removal periods for the whole experiment
 835 (A), wood species (B) and forest classes (C) after 12 months. The 15 tree species are ordered
 836 according to wood density, ranging from the most (bottom) to least dense (top). Filled red dots
 837 indicate the average values. UF_{ENdrought} = Undisturbed Forest; UF_{ENfire} = Burned primary forests;
 838 LBF_{ENdrought} = Forests logged and burned before the 2015-16 El Niño; LBF_{ENfire} = Forests logged
 839 before but burned during the 2015-16 El Niño; Log_{ENdrought} = Forests with selective logging.



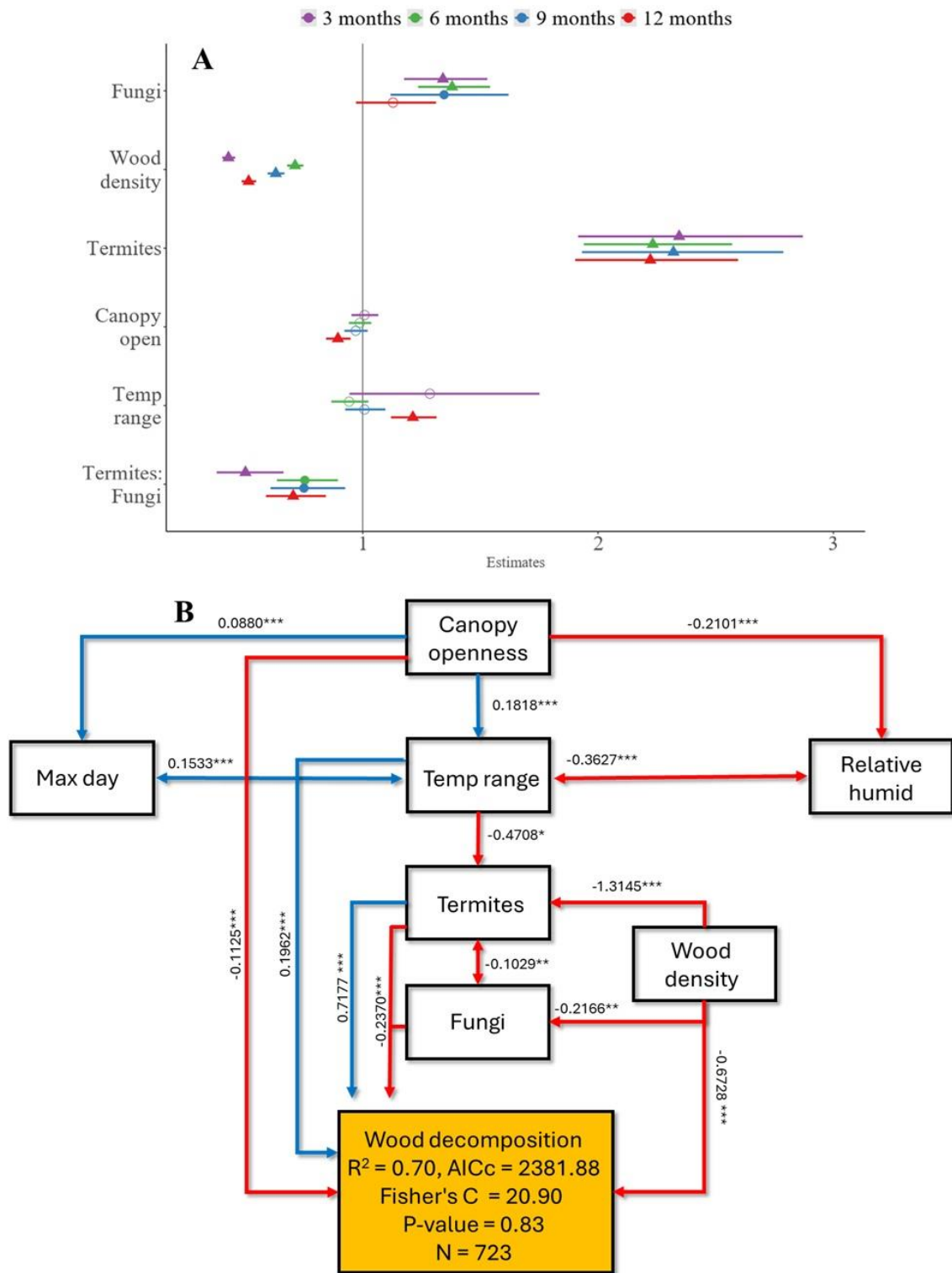
840

841 Fig. 3. Estimates of regression coefficients with confidence intervals for the proportional mass
 842 loss of wood blocks affected by microclimatic and wood density (Q2). The symbols represent the
 843 significance level of the explanatory variable, with those to the left of the central vertical line
 844 indicating negative trends and those to the right indicating positive relationships with the response
 845 variable. Hollow symbols represent non-significant variables ($p > 0.05$). Significance of each
 846 symbol: ■ = $p < 0.001$; ▲ = $p < 0.01$; ● = $p < 0.05$.



847

848 Fig. 4. Odd ratios with confidence intervals for termite (A) and fungi (B) visible presence as
 849 affected by microclimatic factors, wood density and canopy openness (Q3). The symbols
 850 represent the significance level of the explanatory variable, with those to the left of the central
 851 vertical line indicating negative trends and those to the right indicating positive relationships with
 852 the response variable. Hollow symbols represent non-significant variables ($p > 0.05$). Variable
 853 significance of each symbol: ■ = $p < 0.001$; ▲ = $p < 0.01$; ● = $p < 0.05$.



854

855 Fig. 5. Estimates of regression coefficients with confidence intervals for the proportional mass
 856 loss of wood blocks affected by microclimatic, forest structure and biotic factors (A) and
 857 Structural equation model (SEM) reduced over twelve months of study (B). Double-headed
 858 arrows signify the correlated error path between the variables concerned. Blue arrows denote

859 significant positive relationships, while red lines represent significant negative relationships. The
860 standardized coefficients are shown next to each arrow. The fit of the model, including Fisher's
861 C-statistic, the p-value and the corrected AICc value, is shown inside the yellow box. P-value >
862 0.05 represents that the SEM model fits the data, i.e. the covariance matrix of the model does not
863 differ significantly from the observed matrix. Significance of each linear model: *p < 0.05; **p
864 < 0.01; ***p < 0.001.

865

866

867

868

869

870

871

872

873

874

875

876

877

878

879

880

881 **Supplementary material**

882 ****Resumo em português**

883 As florestas amazônicas desempenham um papel fundamental na dinâmica dos serviços
884 ecossistêmicos globais. Florestas modificadas pelo homem, que já cobrem mais de um
885 milhão de km² na região, geram ameaças ainda incertas ao ciclo do carbono, como a
886 influência nas taxas de decomposição da madeira. Compreender os fatores que regulam
887 a decomposição da madeira morta é fundamental para melhorar as previsões do fluxo de
888 carbono em florestas tropicais. Utilizando um experimento de campo padronizado de um
889 ano na Amazônia oriental, considerando 15 espécies de árvores nativas, este estudo
890 avaliou como a perturbação florestal, o microclima, as características da madeira e a
891 atividade de decompositores afetam os processos de decomposição da madeira.
892 Trimestralmente, a decomposição da madeira aumentou gradualmente, atingindo $0,21 \pm$
893 $0,29$ de perda proporcional de massa após 12 meses. A densidade da madeira
894 desempenhou um papel crucial, confirmando-a como um preditor fundamental das taxas
895 de decomposição, com madeiras de menor densidade apresentando maiores taxas de
896 decomposição. Apesar da ausência de diferenças significativas nas taxas de
897 decomposição entre as classes de perturbação florestal, os modelos de equações
898 estruturais revelaram vias indiretas significativas, nas quais a abertura antropogênica do
899 dossel alterou as condições microclimáticas, o que, por sua vez, suprimiu a atividade de
900 decompositores, como cupins, um importante fator biótico da decomposição. Nossas
901 descobertas fornecem novas evidências experimentais de que a estrutura florestal e o
902 microclima mediam o papel dos decompositores na ciclagem do carbono, enfatizando a
903 necessidade de incorporar características funcionais da madeira e efeitos indiretos de
904 perturbação em modelos de carbono para melhor prever as respostas dos ecossistemas
905 sob a crescente degradação florestal e às mudanças climáticas.

906 **Palavras-chave:** Amazônia, decomposição de madeira, extração seletiva, incêndios
907 florestais, cupins, fungos, microclima.

908 Table SM 1. Tree species used for the proportional mass loss standard experiment with wood
909 blocks (n = 3240) in the Santarém region. The wood density average and their respective standard
910 deviations (SD) were obtained by drying to constant mass and calculating the volume by
911 gravimetric water displacement method.

Family	Species	Wood density (g.cm⁻³)	SD (g.cm⁻³)
Bixaceae	<i>Bixa arborea</i>	0.3596	0.0332
Bignoniaceae	<i>Jacaranda copaia</i>	0.4592	0.0408
Araliaceae	<i>Didymopanax_morototoni</i>	0.4819	0.0632
Meliaceae	<i>Cedrela odorata</i>	0.5596	0.0272
Lecythidaceae	<i>Couratari guianensis</i>	0.5611	0.0413
Boraginaceae	<i>Cordia goeldiana</i>	0.6234	0.0452
Vochysiaceae	<i>Qualea dinizii</i>	0.6396	0.0404
Lecythidaceae	<i>Cariniana micrantha</i>	0.6462	0.0467
Lauraceae	<i>Mezilaurus itauba</i>	0.8595	0.0177
Caryocaraceae	<i>Caryocar glabrum</i>	0.8630	0.0893
Anacardiaceae	<i>Astronium lecointei</i>	0.8710	0.0575
Goupiaceae	<i>Goupia Glabra</i>	0.9539	0.0755
Sapotaceae	<i>Manilkara paraensis</i>	1.0181	0.0880
Bignoniaceae	<i>Handroanthus serratifolius</i>	1.0545	0.0459
Fabaceae	<i>Swartzia grandifolia</i>	1.1518	0.0644

912

913

914

915

916

917

918

919

920

921 Table SM 2. Time length of each tree species remained in the oven until they reached constant
 922 mass.

Specie	Oven entrance	Oven removal	Days to reach constant mass
<i>Bixa arborea</i>	01/11/2022	07/11/2022	6
<i>Jacaranda copaia</i>	27/10/2022	11/11/2022	15
<i>Didymopanax morototoni</i>	02/11/2022	14/11/2022	12
<i>Cedrela odorata</i>	26/10/2022	10/11/2022	15
<i>Couratari guianensis</i>	29/10/2022	11/11/2022	13
<i>Cordia goeldiana</i>	27/10/2022	15/11/2022	19
<i>Qualea dinizii</i>	02/11/2022	22/11/2022	20
<i>Cariniana micrantha</i>	31/10/2022	16/11/2022	16
<i>Mezilaurus itauba</i>	28/10/2022	14/11/2022	17
<i>Caryocar glabrum</i>	24/10/2022	12/11/2022	19
<i>Astronium lecointei</i>	25/10/2022	15/11/2022	21
<i>Goupia glabra</i>	29/10/2022	10/11/2022	12
<i>Manilkara paraensis</i>	31/10/2022	02/12/2022	32
<i>Handroanthus serratifolius</i>	28/10/2022	16/11/2022	19
<i>Swartzia grandifolia</i>	06/11/2022	22/11/2022	16

923 Table SM 3. Results of the generalized linear mixed models to test whether microclimatic, wood
 924 density and canopy openness variables explain wood decomposition (Q2). WD = wood density
 925 (g.cm^{-3}); Temp Range = Average temperature range ($^{\circ}\text{C}$); Max day = Average maximal
 926 temperature ($^{\circ}\text{C}$).

Predictors	3 months		6 months		9 months		12 months	
	Estimates	p	Estimates	p	Estimates	p	Estimates	p
(Intercept)	0.03	<0.001	0.09	<0.001	0.15	<0.001	0.18	<0.001
WD	0.39	<0.001	0.62	<0.001	0.54	<0.001	0.45	<0.001
Temp Range	1.03	0.908	1.04	0.54	1.01	0.848	1.15	0.004
Max day	1.08	0.61	0.93	0.535	0.98	0.735	0.9	0.039
Random Effects								
σ^2	0.13		0.18		0.37		0.38	
τ_{00}	0.00 _{plot}		0.02 _{plot}		0.02 _{plot}		0.03 _{plot}	
ICC	0		0.09		0.06		0.06	
Observations	807		810		807		723	
R^2_m / R^2_c	0.873 / 0.874		0.536 / 0.579		0.494 / 0.525		0.613 / 0.637	

927

928

929

930 Table SM 4. Results of the generalized linear mixed models to test whether the prevalence of
 931 observed termite attack is explained by structural, site-specific and microclimatic variables (Q3).
 932 WD = wood density (g.cm⁻³); Temp Range = Average temperature range (°C); Fungi = visible [1]
 933 presence of fungi; Max day = Average maximal temperature (°C); Min night = Average minimal
 934 temperature (°C); Rel humid = Average relative humidity (%).

<i>Predictors</i>	3 months		6 months		9 months		12 months	
	<i>Odds Ratios</i>	<i>P</i>	<i>Odds Ratios</i>	<i>P</i>	<i>Odds Ratios</i>	<i>P</i>	<i>Odds Ratios</i>	<i>P</i>
(Intercept)	0.01	<0.001	0.15	<0.001	2.81	0.001	1.13	0.654
WD	0.27	<0.001	0.22	<0.001	0.24	<0.001	0.26	<0.001
Temp range	0.12	0.068			0.55	0.05	0.63	0.024
Fungi [1]	0.5	0.015			0.37	<0.001	0.58	0.006
Max day			2.82	0.014	1.86	0.037		
Min night			0.66	0.049	0.77	0.153		
Rel Humid			2.92	0.029				
Random Effects								
σ^2	3.29		3.29		3.29		3.29	
τ_{00}	0.62 _{plot}		0.37 _{plot}		0.36 _{plot}		0.68 _{plot}	
ICC	0.16		0.1		0.1		0.17	
Observations	807		810		807		723	
R ² _m / R ² _c	0.291 / 0.404		0.406 / 0.465		0.373 / 0.435		0.335 / 0.448	

935 Table SM 5. Results of the generalized linear mixed models to test whether the prevalence of
 936 observed fungal proliferation is explained by structural, site-specific and microclimatic variables
 937 (Q3). Min night = Average minimal temperature (°C); Rel humid = Average relative humidity
 938 (%); WD = wood density (g.cm⁻³); Termites = visible [1] presence of termites; CO = Average
 939 canopy openness (%).

<i>Predictors</i>	3 months		6 months		9 months		12 months	
	<i>Odds Ratios</i>	<i>P</i>	<i>Odds Ratios</i>	<i>P</i>	<i>Odds Ratios</i>	<i>P</i>	<i>Odds Ratios</i>	<i>P</i>
(Intercept)	0.04	<0.001	0.95	0.873	2.86	<0.001	1.99	0.012
Min Night	0.56	<0.001	1.94	0.001	1.05	0.761	0.84	0.236
Rel Humid	14.97	0.005	2.14	0.035	0.88	0.323	0.95	0.746
WD	0.39	<0.001	0.47	<0.001	0.59	<0.001	0.71	<0.001
Termites [1]	0.53	0.019	0.88	0.528	0.38	<0.001	0.59	0.008
CO	0.9	0.236	0.81	0.053	0.68	0.001	1.01	0.918
Random Effects								
σ^2	3.29		3.29		3.29		3.29	
τ_{00}	0.03 _{plot}		0.38 _{plot}		0.69 _{plot}		0.56 _{plot}	
ICC	0.01		0.1		0.17		0.15	
Observations	807		810		807		723	
R ² _m / R ² _c	0.253 / 0.259		0.170 / 0.256		0.093 / 0.250		0.032 / 0.174	

940 Table SM 6. Results of the generalized linear mixed models to test whether microclimatic, wood
 941 density, canopy openness and biotic variables explain wood decomposition (Q4). Fungi = visible
 942 [1] presence of fungi; WD = wood density (g.cm^{-3}); Termites = visible [1] presence of termites;
 943 CO = Average canopy openness (%); Temp Range = Average temperature range ($^{\circ}\text{C}$).

<i>Predictors</i>	3 months		6 months		9 months		12 months	
	<i>Estimates</i>	<i>p</i>	<i>Estimates</i>	<i>p</i>	<i>Estimates</i>	<i>p</i>	<i>Estimates</i>	<i>p</i>
(Intercept)	0.03	< 0.001	0.06	< 0.001	0.08	< 0.001	0.11	< 0.001
Fungi [1]	1.34	< 0.001	1.38	< 0.001	1.35	0.002	1.13	0.114
WD	0.43	< 0.001	0.71	< 0.001	0.63	< 0.001	0.52	< 0.001
Termites [1]	2.34	< 0.001	2.23	< 0.001	2.32	< 0.001	2.22	< 0.001
CO	1.01	0.795	0.99	0.612	0.97	0.247	0.89	< 0.001
Temp range	1.29	0.111	0.94	0.161	1.01	0.865	1.21	< 0.001
Fungi [1] : Termites [1]	0.5	< 0.001	0.75	0.001	0.75	0.007	0.7	< 0.001
Random Effects								
σ^2	0.13		0.16		0.31		0.33	
τ_{00}	0.00 _{plot}		0.00 _{plot}		0.01 _{plot}		0.01 _{plot}	
ICC	0.01		0.02		0.03		0.03	
Observations	807		810		807		723	
$R^2_{\text{m}}/R^2_{\text{c}}$	0.872 / 0.874		0.682 / 0.687		0.602 / 0.616		0.686 / 0.695	

944

945

946

947

948

949

950

951

952

953 Table SM 7. Kruskal–Wallis tests comparing the microclimate variables in a gradient of
 954 disturbed forests in Santarém region. UF_{ENDrought} = Undisturbed Forest; UF_{ENfire} = Burned
 955 primary forests; LBF_{ENDrought} = Forests logged and burned before the 2015-16 El Niño; LBF_{ENfire}
 956 = Forests logged before but burned during the 2015-16 El Niño; Log_{ENDrought} = Forests with
 957 selective logging.

Forest Class	Three months				Six months			
	Max Temp	Min Temp	Temp range	RH	Max Temp	Min Temp	Temp range	RH
UF _{ENDrought}	25.64	23.22	3.98	99.42	26.06	23.21	5.16	99.13
UF _{ENfire}	25.73	23.23	4.07	99.99	26.53	23.23	6.42	99.21
LBF _{ENDrought}	25.97	23.43	4.08	99.79	26.34	23.50	4.66	99.49
LBF _{ENfire}	26.16	23.45	4.49	99.99	26.70	23.46	6.19	99.24
Log _{ENDrought}	25.60	23.39	3.76	99.99	26.01	23.46	4.71	99.61
KW p-value	< 0.001	< 0.001	< 0.001	< 0.001	< 0.001	< 0.001	< 0.001	< 0.001
χ^2	577.08	338.14	404.13	45.24	552.37	317.24	343.62	188.87

Forest Class	Nine months				Twelve months			
	Max Temp	Min Temp	Temp range	RH	Max Temp	Min Temp	Temp range	RH
UF _{ENDrought}	27.08	23.43	7.51	94.78	27.39	23.58	6.30	96.05
UF _{ENfire}	28.13	23.53	10.35	90.96	28.54	23.68	8.49	93.46
LBF _{ENDrought}	27.54	23.79	8.50	91.23	27.89	24.07	7.19	92.98
LBF _{ENfire}	28.07	23.68	10.03	89.49	28.59	23.90	9.44	89.49
Log _{ENDrought}	27.26	23.81	7.44	94.53	27.84	24.02	7.42	94.48
KW p-value	< 0.001	< 0.001	< 0.001	< 0.001	< 0.001	< 0.001	< 0.001	< 0.001
χ^2	385.62	273.96	452.79	235.3	357.75	266.77	330.14	228.44

958

959

960

961

962

963 Table SM 8. Summary of piecewiseSEM results (fourth block removal – after 12 months) in a
 964 gradient of disturbed forests in Santarém region. Significant ($p < 0.05$) relationships are printed
 965 in bold. Max day = Average maximal temperature (°C); Rel humid = Average relative humidity
 966 (%); CO = Average canopy openness (%); Termites = visible presence of termites; Fungi = visible
 967 presence of fungi; WD = wood density (g.cm-3); Temp Range = Average temperature range (°C);
 968 Proportional Mass Loss = PML.

969 Fisher's C = 20.9; $p = 0.83$; AICc = 2381.89

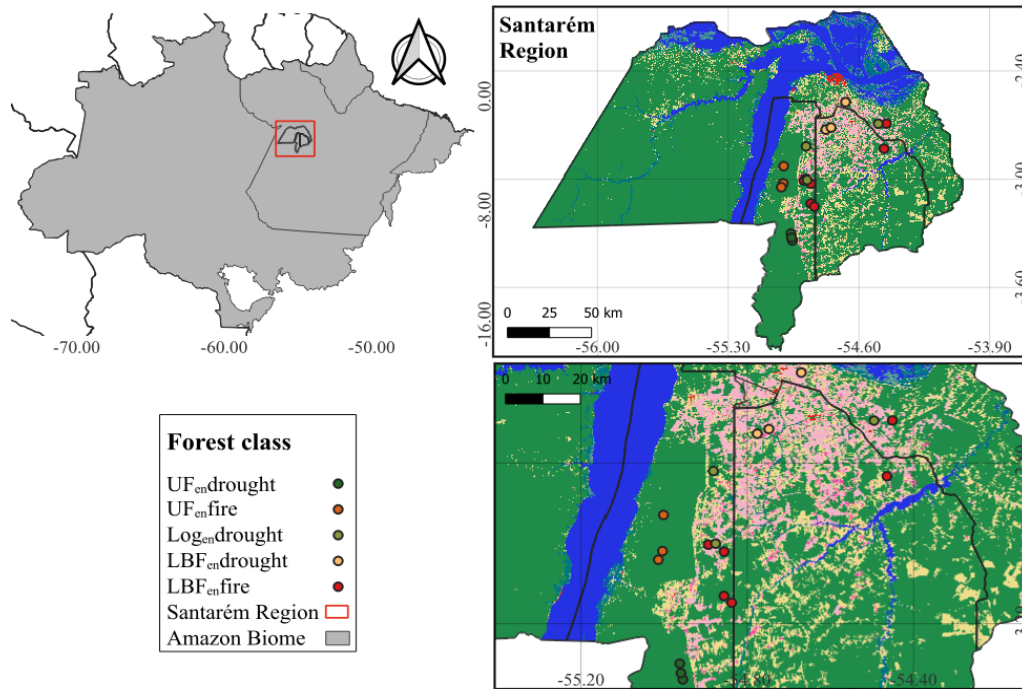
Response variable	Predictor variable	Estimate	SE	P
Max day	CO	0.088	0.0225	< 0.001
Rel Humid	CO	-0.2101	0.0276	< 0.001
	CO	0.1818	0.0228	< 0.001
	Max day	0.1533	-	< 0.001
	Rel Humid	-0.3627	-	< 0.001
Termites	WD	-1.3145	0.1114	< 0.001
Termites	Temp range	-0.4708	0.202	0.0198
Fungi	WD	-0.2166	0.0815	0.0079
PML	WD	-0.6728	0.0299	< 0.001
PML	Termites	0.7177	0.0586	< 0.001
PML	CO	-0.1125	0.0302	< 0.001
PML	Temp range	0.1962	0.0408	< 0.001
PML	Termites:Fungi	-0.237	0.0571	< 0.001
Termites	Fungi	-0.1029	-	0.0028

970

Response variable	R^2
PML	0.70

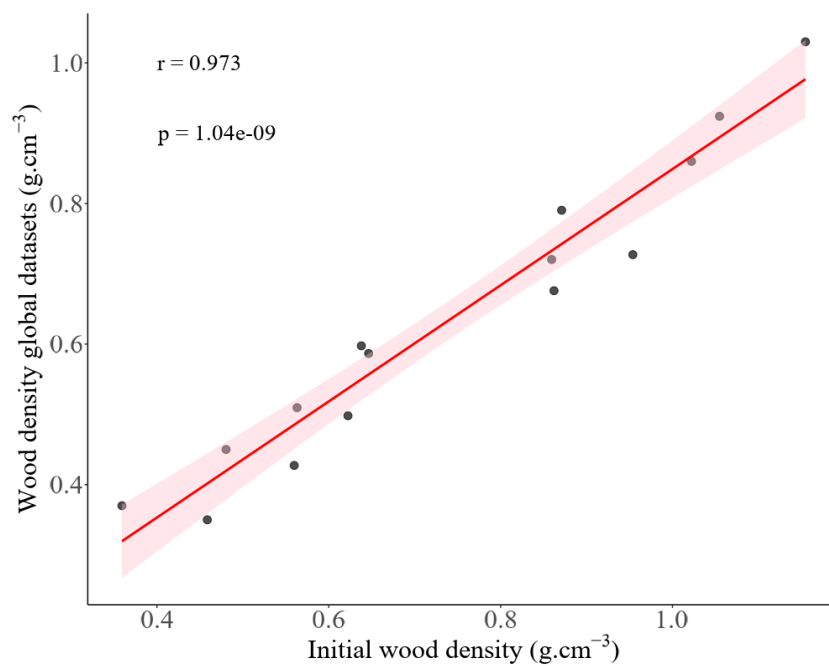
971

972



973

974 Fig. SM 1. Santarém region. Study area consists of 18 transects distributed along a post-El Niño
 975 gradient of forest disturbance. UF_{ENdrought} = Undisturbed Forest; UF_{ENfire} = Burned primary
 976 forests; LBF_{ENdrought} = Forests logged and burned before the 2015-16 El Niño; LBF_{ENfire} =
 977 Forests logged before but burned during the 2015-16 El Niño; Log_{ENdrought} = Forests with
 978 selective logging.



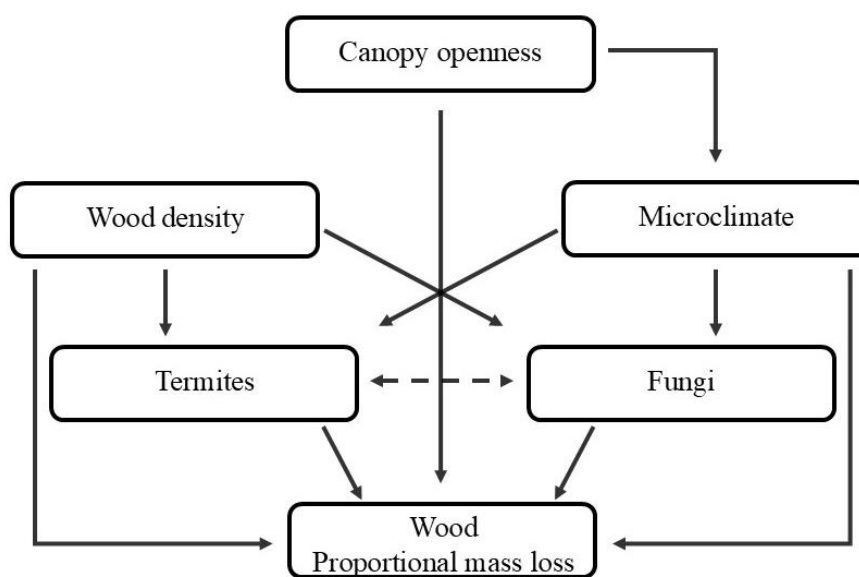
979

980 Fig. SM 2. Pearson's correlation of wood densities and global wood density database (Zanne et
981 al., 2009) of the 15 Amazonian species studied. Shaded area represents the 95% confidence
982 interval of the regression line.



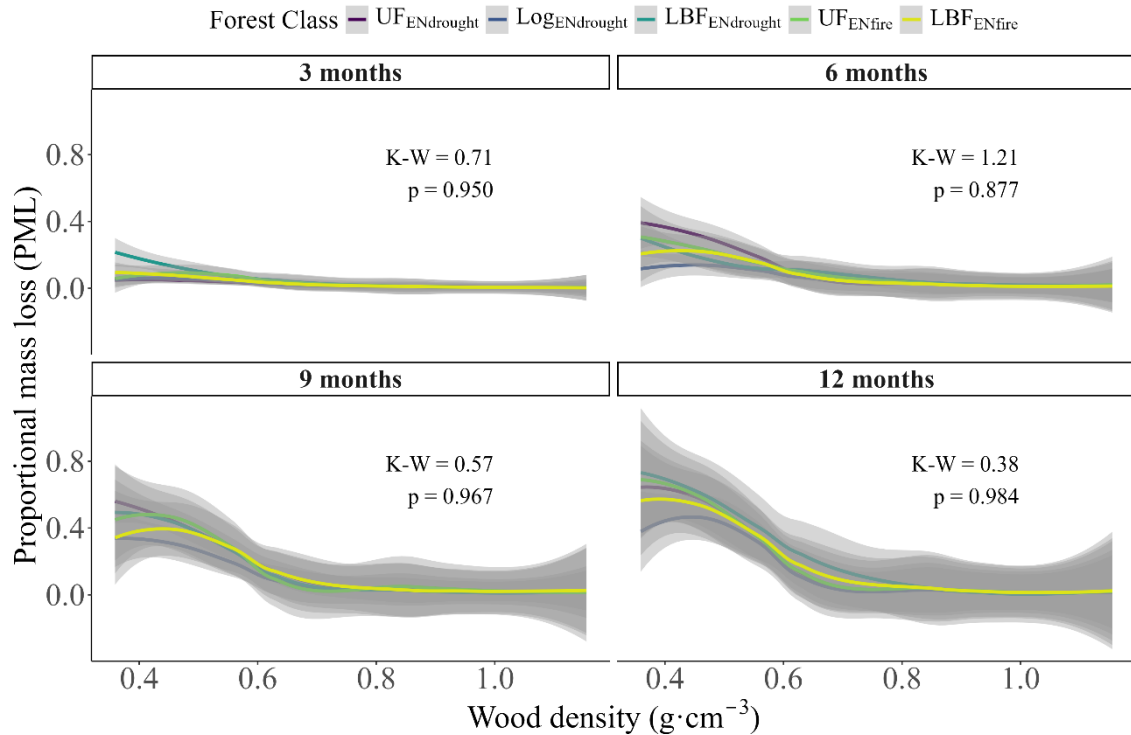
983

984 Fig. SM 3. Design of the collars used in the experiment. In each of the 18 sampled transects, we
985 established three sampling points, located at 0, 150 and 300 m. In each sampling point we installed
986 four collars.



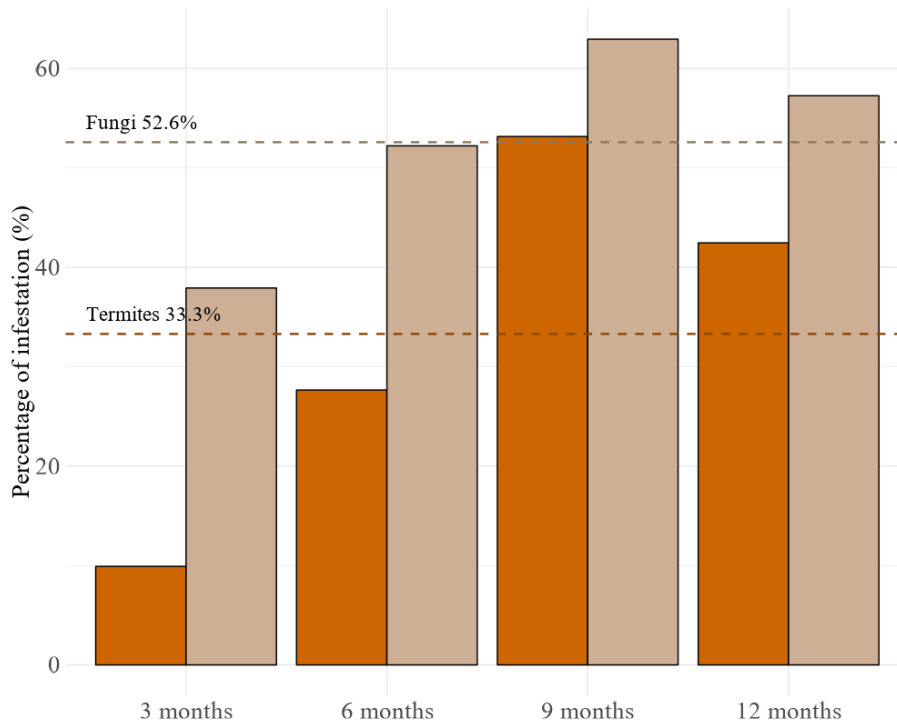
987

988 Fig. SM 4. Conceptual framework of the relationships among forest disturbance, microclimate,
 989 wood traits and decomposers activity with wood decomposition. Direction of single arrows refers
 990 to the hypothesized causal relationships. Double-headed dashed lines refer to a correlative
 991 relationship.



992

993 Fig. SM 5. Relationship between proportional mass loss (PML) and wood density ($\text{g}\cdot\text{cm}^{-3}$) across
 994 four removal periods (3, 6, 9, and 12 months) in each disturbed forest classes in the eastern
 995 Amazon. Lines show the trends with 95% confidence intervals (shaded areas). Kruskal–Wallis
 996 tests were performed using *PML* as the response variable and forest class as the grouping factor.
 997 $\text{UF}_{\text{ENdrought}}$ = Undisturbed Forest; $\text{UF}_{\text{ENfire}}$ = Burned primary forests; $\text{LBF}_{\text{ENdrought}}$ = Forests
 998 logged and burned before the 2015-16 El Niño; $\text{LBF}_{\text{ENfire}}$ = Forests logged before but burned
 999 during the 2015-16 El Niño; $\text{Log}_{\text{ENdrought}}$ = Forests with selective logging.



1000

1001 Fig. SM 6. Percentage of termite (orange) and fungi (peach) infestation throughout the experiment

1002 in the Santarém region. The dashed lines represent the infestation average of the experiment.

1003